University of Catania

Department of Biological, Geological and Environmental Sciences

Ph.D. in Earth and Environmental Sciences

Curriculum Environmental Biology and Biotechnology

XXXV Cycle

Sara Ignoto

Innovative Experimentation of Sea Urchin: *Paracentrotus lividus* (Lamarck, 1816) as model organism

Ph.D. Thesis

Tutor: Prof. Maria Violetta Brundo

Co-tutor: Prof. Bianca Maria Lombardo

Co-tutor: Dr. Roberta Pecoraro

2022/2023

To Giuseppina Messina

and her infinite and contagious passion

"No bird flies as soon as it is born, but the moment comes when
the call of the air is stronger than the fear of falling and then
life teaches it to spread its wings."

Luis Sepúlveda

PREFACE

Sea urchins are emblematic marine organisms to investigate the different areas of biology and ecology; they are widely used as organisms' model in developmental studies due to several similarities with Vertebrate. For the same reason, they are also involved in genetic studies. From the ecotoxicological point of view, sea urchins are useful indicators for environmental contamination due to the fact that their gametes and larval stages are very sensitive to different organic and inorganic pollutants common in coastal marine waters. In Mediterranean waters, *Paracentrotus lividus* (Lamarck, 1816) is highly appreciated for the taste of its gonads (roe), which unfortunately caused an overexploitation of the resource. However, *P. lividus* is not the only edible and highly appreciated sea urchin species worldwide. The aim of this study is: 1. elaborate on the use of *P. lividus* as model organism for the evaluation of coastal water quality and contamination in little studied areas of the eastern Sicily; 2. evaluation of the reproductive period and maturity stages in different areas of eastern Sicily; 3. utilization of *P. lividus* spermatozoa to test new compounds associated to water remediation that soon they will be even more common and abundant in the aquatic environment. In conclusion, the aim of these researches is to provide new data on different aspects of sea urchin, with particular emphasis on its utilization as bioindicator and model organisms, as well as reproductive biology aspect. Concerning this latter point, echinoculture represent a very important goal to reach in order to preserve and protect natural population of this biological resource, unfortunately increasingly rare due to indiscriminate (and often illegal) fishing activities.

CHAPTER 1 - INTRODUCTION

1.1 - Biology and ecology of *Paracentrotus lividus*

1.1.1 - Generalities on *Paracentrotus lividus*: systematic, morphology and anatomy

Paracentrotus lividus (Lamarck, 1816) belonging to Phylum Echinodermata, Class Echinoidea, Order Camarodonta and Family Parechinidae (WoRMS Editorial Board, 2022) (Tab. 1). Echinoderms are deuterostomes and exclusively marine invertebrates with a well-developed coelom and represent one of the most abundant groups among benthic animals, which play a key role in the marine ecosystem (Harrold and Pearse, 1987; Birkeland, 1989; Piraino *et al*., 2002). Another peculiar feature of the echinoderms is the marked pentameral symmetry in the adult stage as opposed to bilateral symmetry in the larval stage. Probably the pentameral symmetry is a secondary adaptation and they evolved from ancestors with bilateral symmetry: this is suggested by some extinct forms without pentameral symmetry (Pawson *et al*., 2010).

The common sea urchin *P. lividus* is a regular echinoid commonly known as purple sea urchin because the colour of some specimens. However, despite its popular name, it presents a high colour variation, from black-purple to red-brown, yellow-brown, light or dark brown and olive green (Fig. 1). In literature it is widely documented that colour does not depend on size, sex, habitat, depth or genetic (Mortensen, 1943; Tortonese, 1965; Boudouresque and Verlaque, 2020).

Classification of *Paracentrotus lividus* (Lamarck, 1816)	
Phylum	Echinodermata
Subphylum	Echinozoa
Class	Echinoidea
Subclass	Euechinoidea
Infraclass	Carinacea
Order	Camarodonta
Infraorder	Echinidea
Family	Parechinidae
Genus	*Paracentrotus*
Species	*Paracentrotus lividus*

Tab. 1. Classification of species *P. lividus* (WoRMS, 2022).

Fig. 1. Colour variation in *P. lividus* species (by Sara Ignoto).

The body of this species has a globular and moderately flattened shape: it shows a robust dermaskeleton that looks like an armour and, together with spines, defends the species against predators. The dermaskeleton consists of a set of calcite plates and ossicles that are attached to each other at sutures by ligaments that wrap around calcite rods (Moss and Meehan, 1967; Asnaghi *et al*., 2019). This structure is called test and can reach dimensions up to 8 cm in diameter (horizontal test diameter without spines) in adult individuals (Boudouresque *et al.*, 1989). This towards the outside gives rise to the primary and secondary spines (also covered by epidermis) which are articulated to the plates by tubercles consist of a basal boss (a low truncate cone) and a terminal knob (mamelon) which articulates with the spine and allowing their movement in any direction. They are robust and pointed, of variable length (not particularly long in this species) but dense and uniformly distributed over the entire surface of the sea urchin test.

Paracentrotus lividus and in general all regular echinoderms, have a pseudo-radiated symmetry, mainly pentameral in the adult individuals. Therefore, it is possible to divide the test into 5 specular parts: each of it consists of a radial area and an interradial area. Each radial area is highlighted by the presence of two rows of pores from which podia (tube feet) emerge; hence these areas are called ambulacrum septa, which are thus distinguished from interambulacrum septa which are devoid of podia (Sartori *et al*., 2017) (Fig. 2).

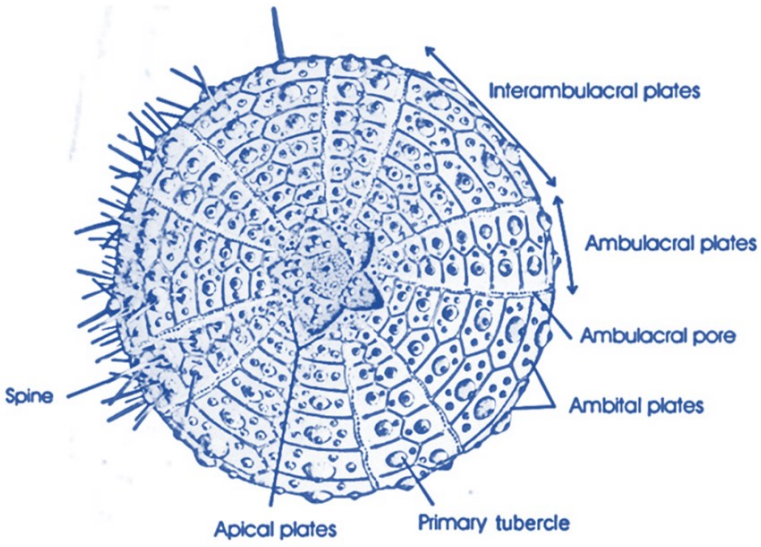

Fig. 2. Ambulacral and interambulacral septa (Modified from Trousset, 1885).

Podia (tube feet) and pedicellariae are particular organelles and are extensions of the water-vascular system. Tube feet in addition to the spines, especially on the hard substratum, have a locomotory function (Fig. 3a). Sea urchin is able to elongate and retract its tube feet: their sucker-shaped tip can glue or unglue it to the hard substratum (Flammang *et al*., 1998) (Fig. 3b).

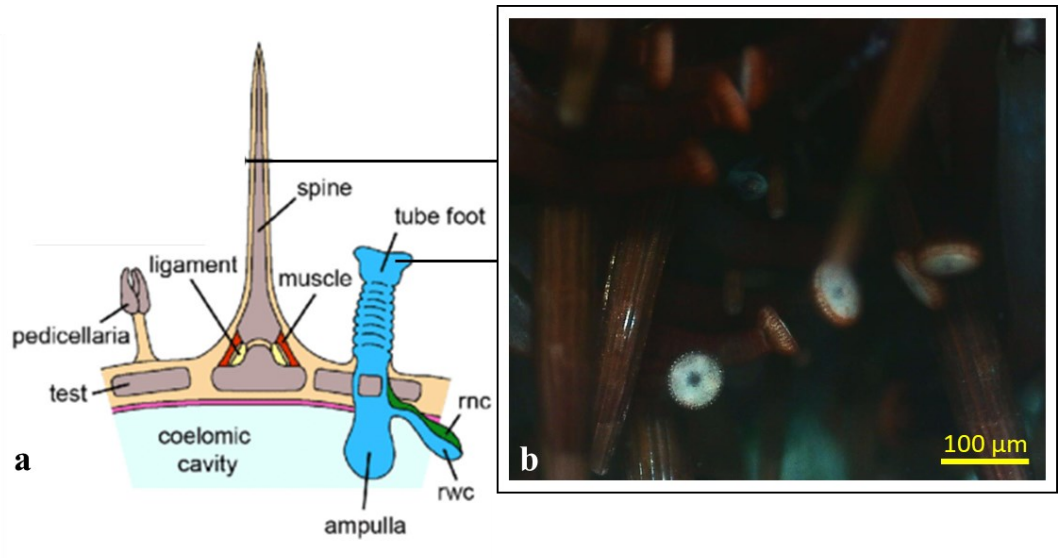

Fig. 3. a) schematic longitudinal section of the test where a spine, a tube foot and a pedicellaria are present (From Ferrario *et al*., 2020); b) spine and tube feet details (by Sara Ignoto).

The pedicellaria have different shapes and functions: rounded used for sensory function (Fig. 4a), while a small pincer-shaped appendage that have tactile and prenhensile function (Fig. 4b). Especially the latter are removing debris from the test surface and covering the test with a various object such as shells, stones and part of aquatic plants for protecting from light and as preventive mechanism of congestion (Pinna, 2014). In fact, this behaviour has been described as "masking" and it has been noted that sea urchins are loaded with more shells when the madreporite (delicate apical opening of their water-vascular system) is in danger of being blocked by sand or particles floating (Richner and Milinski, 2000).

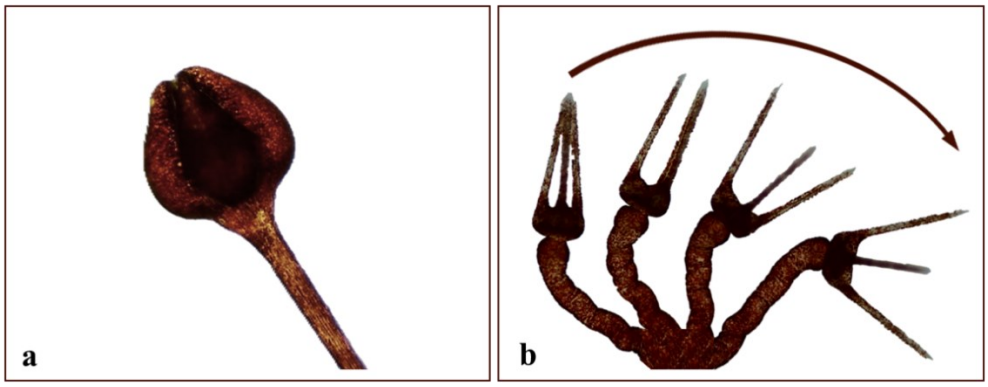

Fig. 4. a) zoom of sensorial pedicellaria; b) details of variation of pincer-shaped pedicellaria (by Sara Ignoto).

The buccal opening and the anus are located in two diametrically opposite surface: oral surface and aboral surface.

The oral surface, always facing downwards, rests on the substrate: in a central position there is the peristome, covered by a thin membrane (peristiomial membrane) that surrounds the typical buccal apparatus of the echinoids which takes the name of Aristotle's Lantern. This is a complex pentasymmetric structure consisting of 5 mobile plates (conical calcite plates, called pyramids) interconnected by more than 40 ossicles; inside on each plate there is a tooth of hard substance, with a pointed end, externally visible on the oral surface. The movements are regulated by a complex of powerful muscles that allow protraction and retraction of the teeth and of all the structure of Aristotle's Lantern (Tortonese, 1965; Barnes, 1987; Devin, 2002; Savriama and Gerber, 2018) (Fig. 5).

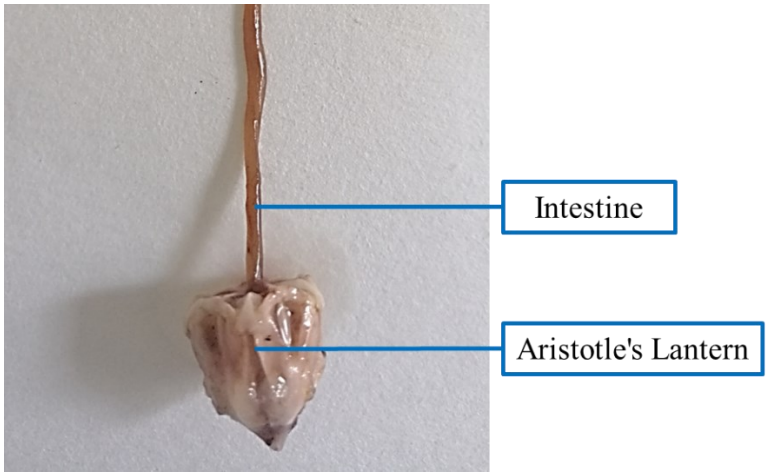

Fig. 5. Aristotle's Lantern and first tract of intestine of *P. lividus* (by Sara Ignoto).

Furthermore, there are 5 pairs of short tube feet (oral tentacles) that surround the teeth and outer edge of the peristomial membrane. There are 5 pairs of branched short pedicels (peristomial gills) without sucker cup which are probably involved in the chemoreceptive and respiration function (Fig. 6).

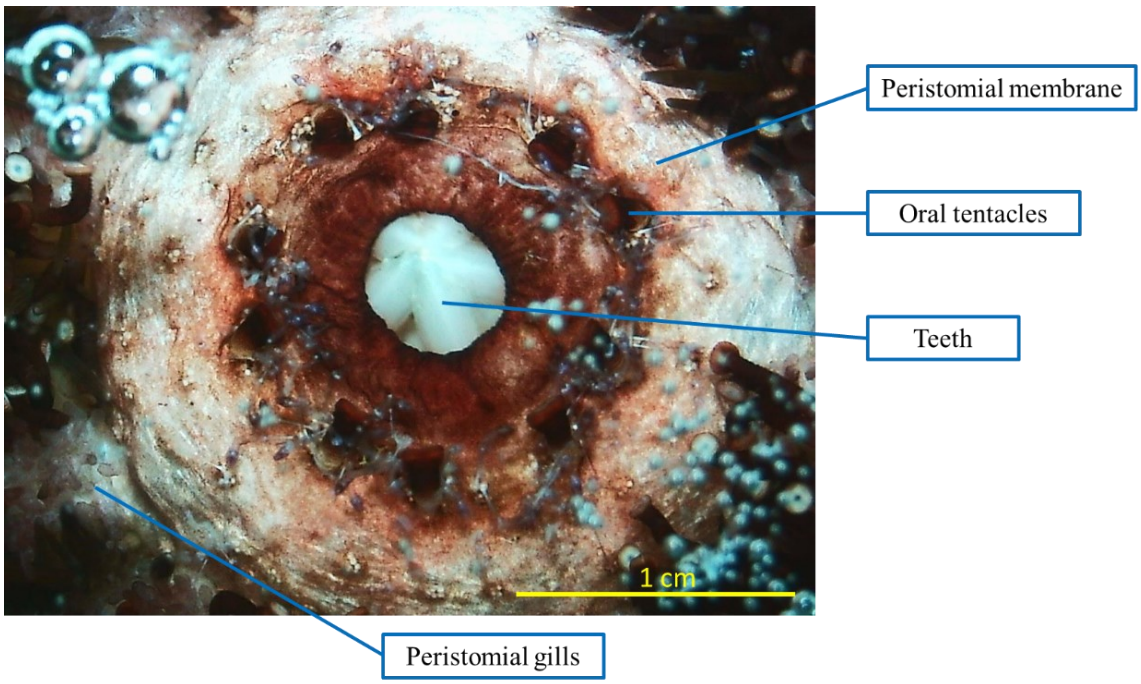

Fig. 6. Detail of the oral surface of *P. lividus* (by Sara Ignoto).

The mouth opens into a long and simple intestine that flows into an anus on the opposite side to the oral surface. At the centre of the aboral surface, there is a membrane named periproct that surround the anus and around this centrale area there is a system of plates: 5 genital plates, where each of them has a hole (gonopore) from which sperms and eggs are released in the water and 5 smaller terminal plates. One of genital plates named madreporic plate in which the madreporite opens, allowing the entry of water by putting the sea urchin in communication with the external environment (Carboni, 2013; Pinna, 2014; Sartori *et al*., 2017) (Fig. 7).

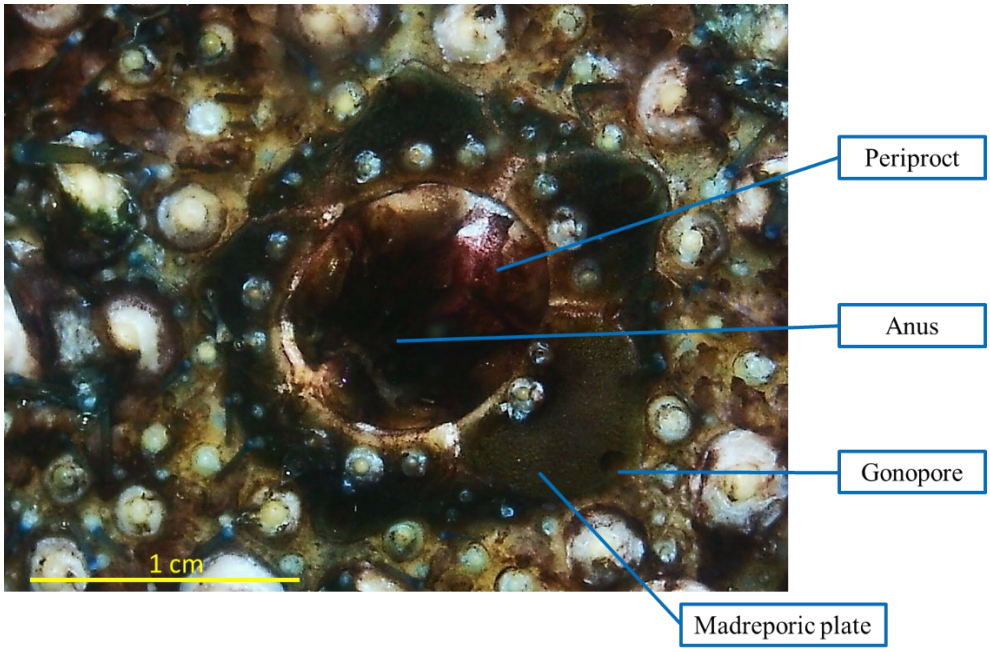

Fig. 7. Detail of the aboral surface of *P. lividus* (by Sara Ignoto).

The celom is well developed and is lined with peritoneum. The water-vascular system is a peculiar apparatus of echinoderms, originates by celom, which is made up of a set of canals that branch out until they project outwards with the podia.

From the external environment, the seawater enters through the opening of the madreporite, crosses the stone canal, that runs through the coelomic cavity in an oral-aboral sense and flows into the ring canal, that surrounds the mouth. From the latter, 5 radial canals branch and run through the respective ambulacral septa carrying the water (endolymph) up to the level of the internal ampullae present at the base of the tube feet. The ampulla-podia systems through the variation of the turgor regulates the swelling of the suction cups at the apex of the tube feet, therefore it is responsible for the locomotion

of the sea urchin. (Fig. 8). In addition to locomotion, the water-vascular system allows the carrying out of respiratory and excretory functions through the pedicellariae (Carboni, 2013).

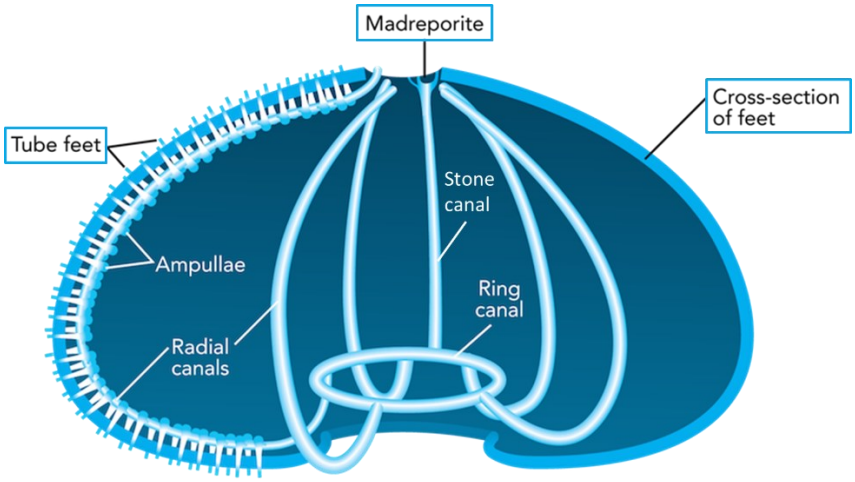

Fig. 8. Scheme of water-vascular system in regular echinoids. Modified from Byron Inouye.

The adult echinoderms' nervous system is composed of a central nervous system made up of a nerve ring connected to a series of radial nerve cords; contains a basiepidermal nerve plexus, a couple of neural condensations, and several peripheral nerves (Kaul-Strehlowet *et al*., 2015; Mashanov *et al*., 2016; Formery *et al*., 2021). Both the central and peripheral nervous systems are composed of complex subdivisions: peripheral nerves extending from the radial nerve cords or nerve ring connect with the peripheral nervous system, located in other organs or effectors including the viscera, podia, body wall muscles, and connective tissue (Díaz-Balzac and García-Arrarás, 2018).

In these organisms, the haemal system is well developed and is structurally and physiologically specialized to perform a series of functions including those involved in the immune defence. It consists of gaps dug between the tissues that run close to the annular canal and the radial canals of the aquifer system. In particular, the haemocoelic structures of the echinoid axial complex include the axial organ, oral haemal ring and extending from it radial haemal vessels, the genital haemal ring and gonad haemal lacunae, and the so-called marginal intestinal vessels. It is also necessary to consider some features of the radial complex of organs, which, in addition to coelomic and haemocoelic components, include nerves and epineural canals (Ezhova *et al*., 2018) (Fig. 9).

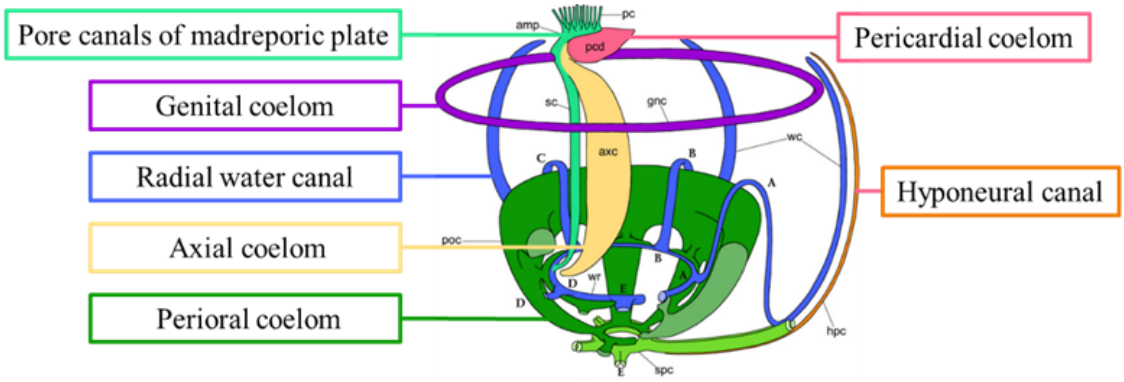

Fig. 9. Scheme of coelomic and haemocoelic components in regular echinoids. Modified from Ezhova *et al.* (2018).

The axial organ is an integral component of the echinoid haemal system; is a large hypertrophy space within the connective tissue matrix, lined by epithelial cells of the coelomic cavities, that attach part of the digestive tract to the calcite endoskeleton. Its anaboral extension is surrounded by the so called dorsal sac and is termed the head process. Axial organ and head process are crossed by numerous anastomosing haemal lacunae that aborally join with the anal haemal ring and the genital lacunae. In addition, the axial organ is crossed by numerous canaliculi that constitute invaginations of the axial coelom and somatocoelomic epithelia; this organ does not end entirely blindly but extends into the perioesophageal haemal ring either directly or through connecting haemal lacunae (Ziegler *et al.*, 2009) (Fig. 10).

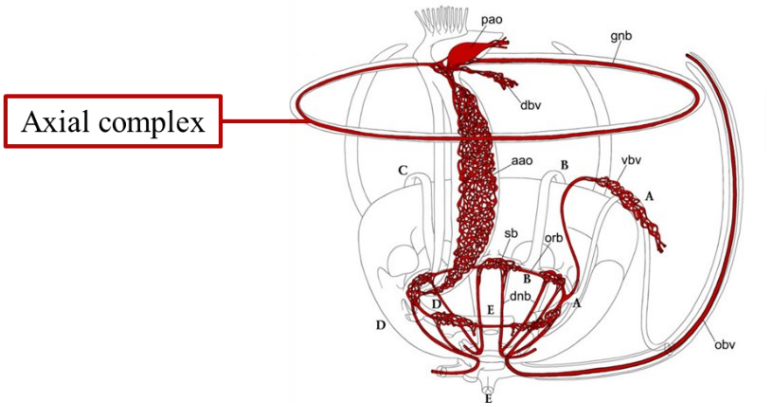

Fig. 10. Scheme of components of axial complex in regular echinoids. Modified from Ezhova *et al*. (2018).

Furthermore, it has recently been stated that the axial complex is undoubtedly the excretory organ of the echinoderms, homologue of the heart-kidney of Hemichordata. The blood network of the axial complex is represented by the system of haemocoelic spaces, which lie between the folds of the coelothelium of axial coelom.

The heart which is enclosed into the pericardial coelom on the aboral side of the body and accepts the blood from two aboral haemal rings: the gastric ring and the genital ring. Its contractions provide directional movement of the blood which is conveyed into the haemocelic gaps of the axial organ; these are separated from the coelom by the basal lamina. This lamina is covered by the coelothelial lining, which contains the podocytes and epithelial-muscle cells. The last type of cells creates the pressure, which provides the ultrafiltration of liquid from the haemocoel to the axial coelom. The coelomic liquid with the products of excretion is removed from the axial coelom to the environment via the pores of madreporic plate (Ezhova and Malakhov, 2021).

Inside the coelomic cavity flows the coelomic fluid which contains sea water with traces of protein and non-protein nitrogen (urea or ammonia), a high concentration of potassium ions, small amounts of lipids and contains several coelomocyte types and molecules involved in innate immune defences (Chia and Xing, 1996). The innate immunity of echinoderms is usually divided into two broad categories: cellular and humoral immunity. Coelomocytes mediate the cellular responses to immune challenges through phagocytosis, encapsulation of non-selfparticles, cytoxicity and the production of antimicrobial molecules (Arizza *et al*., 2007; Schillaci *et al*., 2010; Chiaramonte *et al*., 2019). In addition, a variety of humoral factors found in the coelomic fluid, including lectins, agglutinins, and lysins are important in host defence against pathogens, foreign substances and potentially toxic chemicals (Hibino *et al*., 2006; Smith *et al*., 2010; Arizza *et al*., 2013).

The digestive system is a simple pipe, attached to the inner wall of the body by means of the mesentery. It consists of the mouth, pharynx, esophagus and stomach, intestine and anus: at first, it passes through the Aristotle's lantern, proceeds in its centre among the pyramids and, after folding several times, it ends with the anus (Fig. 11). In the stomach there are exocrine cells suitable for the production and secretion of enzymes and also has numerous enterocytes, usually well developed (Pinna, 2014).

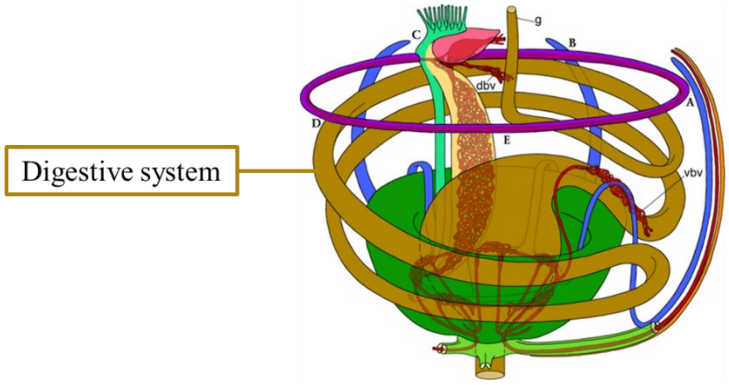

Fig. 11. Scheme of tracts of digestive system of regular sea urchins and other coelomic components. Modified from Ezhova *et al*. (2018).

1.1.2 - Reproduction

Sea urchins are dioecious species: male and female sexes are separate. However, a part of population can present hermaphroditism (Gago *et al*., 2003). In regular sea urchins, eggs and sperm are released from five gonads and respective gonopores lying on the underside of the mouth (aboral surface) (Fig. 12).

Fig. 12. Gonads of *P. lividus* in evidence and Aristotle's Lantern (by Sara Ignoto).

They are mass spawners and release their gametes in the water column (external fertilizers). The size at sexual maturity varies between 2-4 cm in test diameter depending on the geographical area and habitat (Lozano *et al*., 1995; Ouréns *et al*., 2013). When males release their sperms in water, females release millions of very small jelly-coated eggs. Only a percentage between the 10% and 40% of eggs will be fertilized. When the sperm makes contact with the egg surface, the sperm's plasma membrane and the acrosomal membrane fuse together and acrosomal enzymes are released, digesting the egg's jelly coat. Subsequently the nucleus of the sperm is released into the egg. The first organ formed on the larvae is the anus, and then comes the mouth (Formery *et al*., 2022). The sexual maturity is reached at about 3 years (Turon *et al*., 1995).

1.1.2.1 - Sexual dimorphism

Paracentrotus lividus is a gonochoristic species without a clearly visible sexual dimorphism. Indeed, in males, they have been observed genital papillae on the aboral surface. In males, these structures are conical protuberances, while in females they are flattened (Tahara *et al*., 1958; Tahara *et al*., 1960). Sugni *et al.* (2010) were the first to demonstrate the presence of sexual dimorphism in *P. lividus*, describing morphologically and histologically the genital papillae: males presented a short conical papilla, internally lined by a ciliated epithelium, whereas females presented a flattened papilla, slightly sunken in the body surface and without ciliation. From my observations, the genital papillae facilitate the emiction of gametes in correspondence of the gonopore through a series of small contractions, modifying their shape after the emission of gametes (Fig. 13).

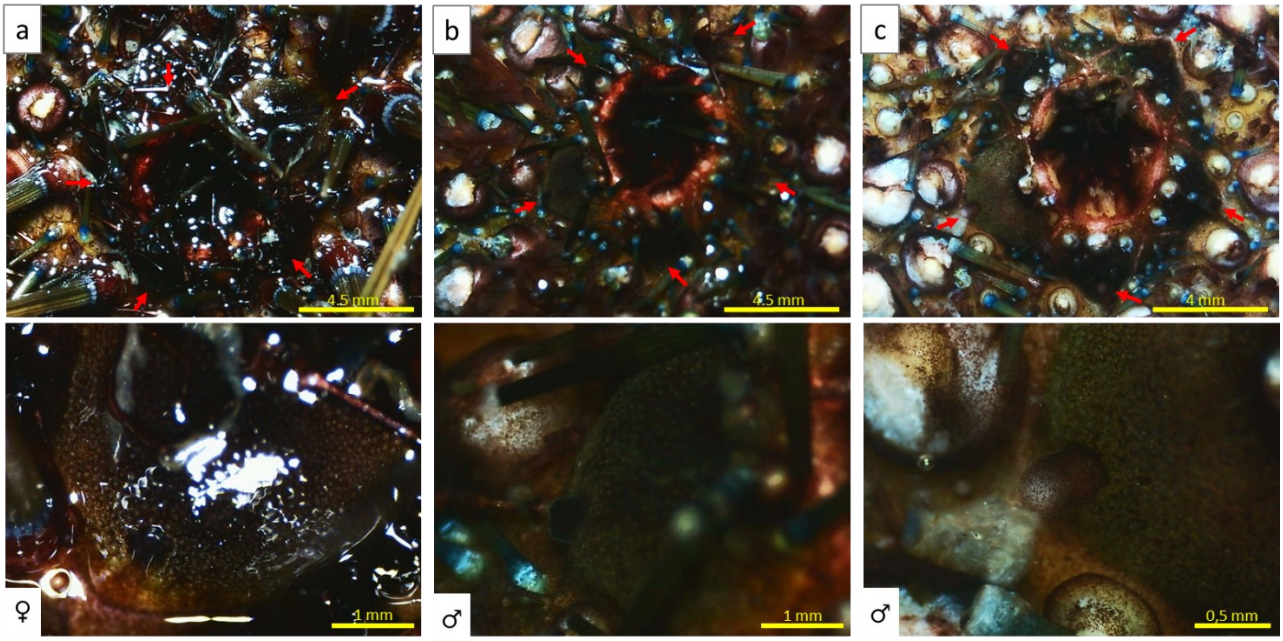

Fig. 13. Genital papillae in *P. lividus*: a) genital papillae in female (red arrows) with detail of the flattened papillae below; b) genital papillae in male (red arrows) and detail of papillae below; c) genital papillae in male post-spawning (red arrows) and one of the elongated papillae in detail below (by Sara Ignoto with NIKON SMZ745).

This could explain the histological and morphological differences observed in the papillae between adult and juveniles, and between reproductive and non-reproductive period. A recent study pointed out the attention on these morphological differences and on their correlation with the diameter of the test in *P. lividus* (Brundu *et al*., 2023). This discovery assumes particular importance for sex identification in laboratory in those experimental contexts because this technique can be easily applied (examined under a stereomicroscope) and allow a fast identification of breeders. It can be

used for in vitro fertilization, echinoculture and non-invasive tool for in vivo sex recognition for example in ecological studies (Sugni *et al*., 2010; Brundu *et al*., 2023).

1.1.3 - Life cycle and embryonal development

When gametes are mature, they are released in the external environment (external fertilization). Embryos are optically transparent and develop in a cone-shaped echinopluteus larva. Six hours after fertilization, the embryo enter in the blastula phase (Davidson *et al*., 1998) (Fig. 14).

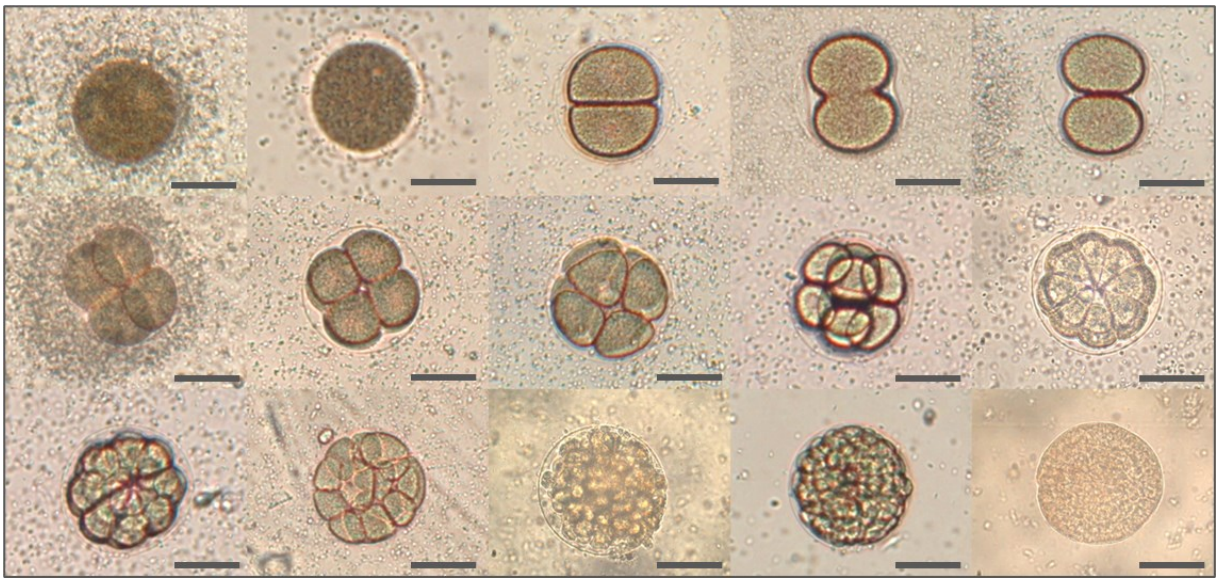

Fig. 14. Table of the sequence of embryonal development of *P. lividus* (by Sara Ignoto with LEICA DMLB). Scale bar =100 µm.

The embryo starts to flatten and the contact area of the SMC (secondary mesenchymal cells) (Fig. 15 a,b,c) in the animal pole starts to invaginate forming the mouth (stomodeum), thus the prism stage (Fig. 15 d,e) is reached. Subsequently, the echinopluteus larva, or simply pluteus, differentiates two days after fertilization. The circumoral region gives rise to four lobed expansions, the arms, supported by calcareous skeletal spicules and at this stage the embryos have become planktonic larvae (Fig. 15 f,g,h) which begin to feed and which are equipped with a fully differentiated skeleton, a digestive system, contractile cells and nervous. The plutei can swim by rotating on themselves thanks to the beats of the eyelashes, located both on the arms and in the circumoral region, coordinated by a kind of nervous system (Garner *et al*., 2016).

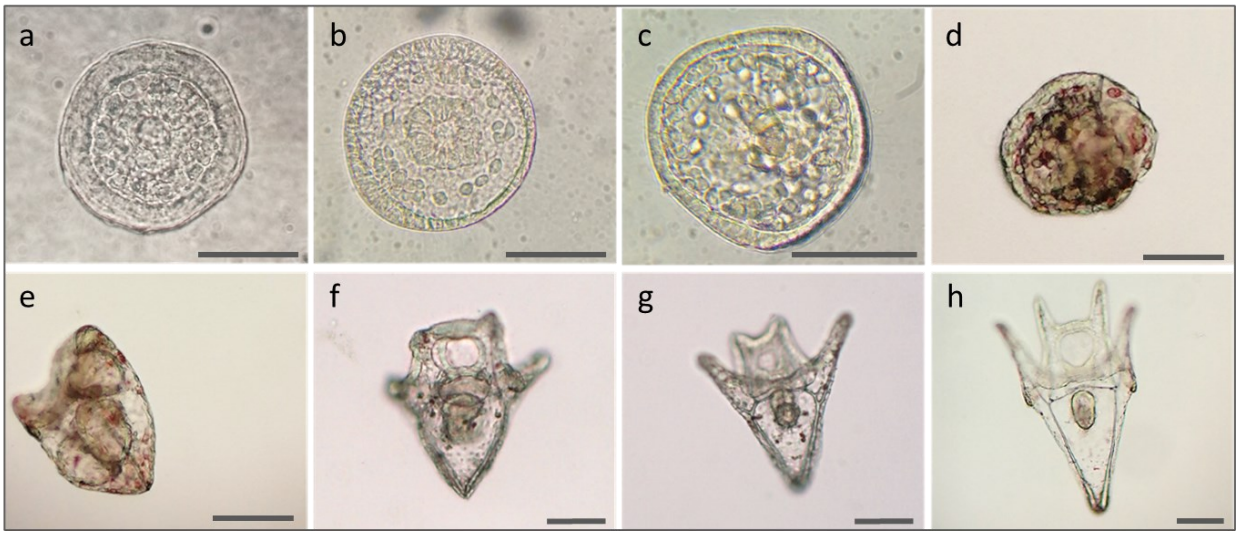

Fig. 15. Table of the sequence of larva development of *P. lividus* (by Sara Ignoto with NIKON E200). Scale bar = 100 µm.

The planktonic larvae are characterized by bilateral symmetry and can live from 20 to 40 days before attaching themselves to the substrate and triggering the metamorphosis process which essentially consists of a phase of evagination and reabsorption of the larval tissues and is completed in about an hour. The resulting post-larval stage is short and lasts only about 8 days, but it is very active from an organogenetic point of view, in fact, at the end of this stage the individuals will have acquired the ability to move and feed (Gosselin and Jangoux, 1998). The adult form has five-radial symmetry.

1.1.4 - Ecology and distribution

The sea urchin *P. lividus* is an edible echinoid whose distribution extends from the Mediterranean Sea (where it is widespread) to the northeastern Atlantic (from Scotland to southern Morocco) (Tortonese, 1965). However, being the most exploited echinoid species in Europe, in some areas local stocks have collapsed as consequence of overexploitation and illegal fishing activities. This fact is particularly serious if we think that this species covers an important ecological role for the sublittoral ecosystem (Rakaj *et al*., 2021). Indeed, *P. lividus* is a gregarious and voracious generalist herbivore, as well as a prey for several fish species, mollusks and starfish. Fishes belonging to the Sparidae family, such as *Diplodus sargus* and *Diplodus vulgaris,* and the Labridae *Coris julis* were observed to be the main predators of *P. lividus*. However, also other species, such as *Labrus merula* and *Thalassoma pavo* can have a relevant role as predators of the species (Sala, 1997). However, most works focused on fishes as predators of *P. lividus* and little attention was paid to other organisms (Savy, 1987). In some locations and conditions, for example, it was demonstrated that the starfish

Marthasterias glacialis can be the major source of mortality for *P. lividus* (Bonaviri *et al*., 2009). Also, the abundance of microinvertebrates can affect mortality rate of settlers of *P. lividus*; indeed, several species were identified as potential predators of this stage of *P. lividus*. In particular, the hermit crabs *Calcinus tubularis* and *Pagurus anachoretus* preyed upon the sea urchins offered; *Pilumnus* spp. and *Liocarcinus arcuatus* consumed most of the sea urchins offered (Bonaviri *et al*., 2012). Hence, also the presence and abundance of micropredators may affect *P. lividus* populations. In some areas and in particular conditions, *P. lividus* can cause the removal of large algal biomass and associated fauna, changing the habitat scenario of relatively extended areas in a short period of time (Kitching and Thain, 1983; Boudouresque and Verlaque, 2020). The species inhabit shallow coastal waters, from 0 to about 20 m deep. It can be mainly found on rocky bottoms and *Posidonia oceanica* meadows (Nédelec and Verlaque, 1984). However, in this latter habitat, it usually reaches lower densities (Sala *et al*., 1998). The reproductive cycle of the species shows an annual pattern: gonads develop during summer and autumn and specimens with mature gonads can be found all the winter. The peak of the spawning period falls between spring-beginning of summer, driven by phytoplankton density, and a secondary less intense event in autumn (Lozano *et al*., 1995); although winter events or prolonged spawning periods have also been recorded (Guettaf *et al*., 2000; Murillo-Navarro and Jiménez-Guirado, 2012).

1.2 - *Paracentrotus lividus* as a valuable resource

1.1.3 - Exploitation, harvesting and echinoculture

In last years, the worldwide supply of sea urchins has considerably diminished (Stefansson *et al*., 2017). At current prices the global market demand for sea urchins is estimated at ~65,000 tonnes, although landings are in all likelihood underestimated. Prices for sea urchins are dependent of several factors (James *et al*., 2017):

- Appearance, colour and quality
- Species and region of harvest
- Flavours and textures
- Demand and distribution
- Form and processing

The gonads of *P. lividus*, that represent the edible part of the species, were already appreciated in the ancient world of the Mediterranean Sea, where they were considered a seafood delicacy by the ancient Greeks. Even today, the reddish-orange gonads of *P. lividus* are highly appreciate in many Mediterranean countries, including Italy (southern part in particular), where they are sometimes called "red gold" to indicate the delicacy and value of this biological resource. In Italy, in the common jargon, the species is called "riccio femmina" (female sea urchin), because most people believe that the edible part of the species is represented by eggs only, so they are convinced that males are not edible and wrongly call "riccio maschio" (male sea urchin) both female and male specimens of *Arbacia lixula*, another common species of sea urchin sympatric with *P. lividus* and considered not good to eat, although also its gonads are edible. Nowadays, in Europe, the value of the gonads of this echinoid can reach 150 euros per kilo (Carboni *et al*., 2012; Sartori and Gaion, 2016). Main consumers of *P. lividus* are France, Spain and Japan, followed, to a lesser extent, by Italy and Greece (Bertocci *et al*., 2018) (Fig. 16).

Fig. 16. Gonads of *P. lividus* at the fish market (by Sara Ignoto).

However, the growing demand of this delicious resource is the cause of the overexploitation present in several Mediterranean areas, in which the species has greatly reduced in abundance or has even disappeared as consequence of illegal and/or uncontrolled fishing activities. For this reason, several research centers are looking for the solution in the aquaculture of the species, that seems to be a promising solution. However, at the current knowledge status, the main limiting factor for reaching an effective production is the lack of adequate feeds for feeding larvae, fast growth of adults and gonadal maturation (Bartley and Bell, 2008; Zupo *et al*., 2019). Hence, for cost-effective production systems in echinoculture requires further investments and efforts to better understand dietary requirements for both larval planktonic and adult benthonic life stages (Fernandez and Boudouresque, 2000). Indeed, during the metamorphosis and growth of the species the body size increase of the species requires variation in feeding (e.g. different levels of protein/carbohydrate ratio). In this context, the modern echinoculture is focusing attention in producing formulated diet mixing different proportions and ingredients of vegetable and animals, reducing the time to produce marketable high-quality gonads (Vizzini *et al*., 2019).

1.2.1.1 - Potential risks for human health

Similarly, to some bivalve mollusks, sea urchin gonads can be a risk for infection to consumers if faecally contaminated, because they are consumed raw. In sea urchins, the food safety is governed by regulations EC No 853/2004 and 854/2004 and rely on *Escherichia coli* presence only. This bacterium is routinely used to test microbiological quality and to classify harvesting areas in different quality levels: A, B and C. However, also other pathogens, such as Norovirus (NoV) and hepatitis A virus (HAV) can be a threat for human health. Indeed, for example, the presence of NoV and HAV in bivalve mollusks has been widely reported (Bazzardi *et al*., 2014; La Bella *et al*., 2017). Nevertheless, the presence of these latter pathogens in *P. lividus* gonads from faecal contamination has not been given attention despite the gonads are usually consumed raw. However, a recent study pointed out the attention of this aspect, showing from specimens sampled in Portugal sure levels of contamination of *E. coli* and *Salmonella* spp., while contamination from NoV was of public health concern (Santos *et al*., 2020a). Considering the bioaccumulation of persistent pollutants in gonads of *P. lividus*, polycyclic aromatic hydrocarbons (PAHs), insecticides, pharmaceuticals and personal care products (PCPs) and flame retardants were found, though in general at low levels and with higher level in more urbanized areas (Angioni *et al*., 2014; Rocha *et al*., 2018). Also, in some areas relevant

bioaccumulation levels of As, Cr, Ni and Pb was recorded in sea urchins living along coasts with high level of anthropogenic activities or in areas with natural geochemical anomaly (Scanu *et al*., 2015).

Also, a recent study demonstrated that "heavy rare earth elemens" (HREEs) are associated to deleterious effects in early stages of *P. lividus*. For example, the exposition of *P. lividus* sperm to HREEs caused decrease of fertilization success (Oral *et al*., 2017).

1.2.2 - Source of biomaterials

Some studies demonstrated the potential of the non-edible body parts of *Paracentrotus lividus* as biomaterials. For example, the peristomial membrane (PM) of *P. lividus* is mainly composed by mammalian-like collagen that represents a potential source of collagen, easily obtainable (and low-cost) from food industry where it represents a waste product. Relatively recent researches suggested that the collagen from sea urchins is a good candidate source for mechanically resistant biomedical devices (Di Benedetto *et al*., 2014; Ferrario *et al*., 2017; Zilia *et al*., 2021;). Another study investigated the fatty acids component in *P. lividus* shell, demonstrating the presence of several fatty acids and esters for potential future application in nutrition and medical use (Salvatore *et al*., 2019). Furthermore, the species could be utilized as source of calcium carbonate for aquaculture.

1.3 - *Paracentrotus lividus* as a model organism

1.2.1 - Ecotoxicological studies

A model organism is a species used to study specific biological process. These organisms show similar genetic characteristics to humans and are used in different areas of biology, such as genetics, developmental biology and neuroscience. Model organisms must have certain characteristics, such as a fast growth, high fecundity and small sizes (Leonelli and Ankeny, 2013).
Paracentrotus lividus is one of the species largely used as model organism, and is used in several fields, such as molecular biology, cellular biology and developmental biology. The reasons that make this species highly appreciated as model organism are several: mature/reproductive specimens can be found in a long period of time during the year; it is relatively simple to maintain it in thanks; fertilization can be easily inducted through different stimulus. Fertilization and developmental tests with sea urchins in general are now included in biological test used for the monitoring of marine

pollution of the International Council for the Exploitation of the Sea (ICES, 1997) (Sartori *et al*., 2017).

The embryo-larval bioassays with marine invertebrates is one of the biological tools used for the evaluation and monitoring of marine pollution worldwide (Paredes and Bellas, 2015). The Water Framework Directive (WFD) establishes a single framework for water protection and management in the EU, with the ultimate objective of achieving good chemical and biological status throughout rivers, lakes, groundwater, estuaries and coastal waters, up to one nautical mile from the coast (Directive 2000/60/ EC). The Marine Strategy Framework Directive (MSFD) focuses on achieving the good environmental status of marine waters up to the limit of jurisdiction of each Member State of the EU (Directive 2008/56/EC). In this context, the use of ecotoxicological bioassay using cryopreserved sea urchin embryos in marine quality assessment can be helpful (as well as fertilization and development in general, being this species sensitive to environmental changes). In the study conducted by Paredes and Bellas (2015) it was demonstrated that the use of cryopreserved sea urchin embryos (*P. lividus*) can be successful used for the evaluation of organic and inorganic pollutants in marine environment. The same authors (Bellas and Paredes, 2011) had already suggested the potential application of cryopreserved sea urchin blastulae for potential application in water quality assessment. The use of *P. lividus* embryos was also applied for the evaluation and quantification of thermal stress (climate changes) and exposure to anthropic contaminants (Ruocco *et al*., 2016; Martino *et al*., 2021). Also, the detection of morphological anomalies in the early development stages of *P. lividus* caused to exposure to environmental stressors are used as biomarker in ecotoxicology (Gambarella *et al*., 2021). Sea urchins allow us to have an idea/estimation of risks to human health because they share with higher organisms, human included, mechanisms driving the development and differentiation (Qiao *et al*., 2003). The exposure to different contaminants and multiple stressors is attributable to similar dose-dependent mechanisms of interference in cell-to-cell communication driven by intracellular or intercellular alteration. These effects are measurable through different morphological anomalies in *P. lividus* developmental stages (Gambarella *et al*., 2021). While the acute exposure to contaminant often causes an immediate lethal effect of irreversible anomalies, the effect of subacute exposure is observed over longer times (ca. 10 days) and not at the first developmental stages. The time of apparition of effects is dependent by the concentration of toxic compounds (Carballeira *et al*., 2012): at higher level of toxic compounds the effect appears in early stages.

1.2.1 - Cryopreservation studies

Cryopreservation is a technique that allow long-term preservation and storage of living biological material at low temperatures (Gao and Critser, 2000). Pioneering researches of Polge *et al*. (1949) demonstrated that the addition of glycerol enabled sperm of several species to survive freezing and thawing. Subsequently, cryopreservation techniques were adopted for gametes and embryos of a number of species. In the first phase of development, the cryopreservation protocols have been adopted mainly on domestic species of commercial interest, but subsequently, in more recent times, an increasing of protocols for cryopreservation of gametes, embryos and larvae of marine invertebrates have been developed (Agca and Crister, 2002; Martinez-Paramo *et al*., 2017).

Considering the great scientific interest in sea urchins as model organisms for developmental biology studies, gametes interactions and for the assessment of marine pollution (Paredes and Bellas, 2015), the cryopreservation of gametes of these species is one way of overcoming problems linked to availability of gametes year-round (Fernandez and Beiras, 2001; Rast *et al*., 2006; Vacquier, 2011). However, to date, no successes were recorded in post-thaw oocyte survival in sea urchins.

The cryopreservation can be divided in five fundamental steps (Paredes *et al*., 2019):

1. Equilibration with one or more cryoprotective agents (CPAs). Several chemical agents have been shown to possess cryoprotective properties. These include membrane-permeating and non-permeating agents. The formers are generally with a lower molecular weight than the former.
2. Cooling. Two main methods are generally used to freeze cells: controlled slow cooling and vitrification.
3. Storage in liquid nitrogen at – 196°C. Generally, the storage of cells at low temperatures does not affect their viability. Cell viability remains stable at low temperatures because liquid water, essential for most metabolic and biosynthetic reactions, does not exist below -130°C.
4. Thawing from sub-zero temperatures. Faster thawing is in general preferred because better. It is usually performed by immersion in water bath or in air at ambient temperature.
5. CPA removal. Because CPAs are toxic, it is important to remove or dilute the solution enough to achieve a final concentration under the toxicity threshold to avoid damage. This step is very delicate.

Several researches conducted on different species of sea urchins have shown a considerable variability in the success of cryopreservation protocols (Paredes *et al*., 2019), with fertilization rates ranging from 6% to 96%. In *P. lividus* it was shown that the addition of sugar trehalose (0.04 M) improves the fertilization rate and survivorship of post-thawed *P. lividus* early life stages (Fabbrocini *et al*., 2014).

Concerning the cryopreservation of sea urchin embryos, it has been carried out with various degrees of success depending on the species, and the developmental stage (Asahina and Takahashi, 1978, 1979). Cryobiology has been carried out on 11 regular sea urchin species, most of which are intertidal species (Paredes *et al*., 2019). However, only a few studies were conducted on oocytes and results are inconclusive. But this is common in marine invertebrates, where oocytes of most species have proven to be exceptionally difficult to cryopreserve (Tervit *et al*., 2005). Indeed, oocytes are very sensitive to the toxicity of cryoprotecting agents, even at lower concentrations than those required. Furthermore, they are also chilling-sensitive and even near zero temperatures can be lethal.

CHAPTER 2 - *PARACENTROTUS LIVIDUS* AS A BIOINDICATOR OF WATER QUALITY

2.1 - Abstract

The concentration of heavy metals in the gonads of the sea urchin, *Paracentrotus lividus* (Echinodermata: Echinoidea), was determined. Samples were collected from three sites in the eastern coast of Sicily (Ionian Sea): S1 – Lago Ganzirri (ME); S2 – Ognina (CT); S3 – Natural Reserve of Vendicari (SR). The specimens examined were purchased from local fishermen (only a Vendicari with authorization) and were intended for human consumption except for the samples taken from the reserve of Vendicari, which represent the experimental control sample. Evaluation of the state of gonads was performed by different analysis (GI and GMI) and by imageJ analysis (PI_1 and PI_2). In a few specimens collected in S1 a pathology was histologically detected. From analysis of heavy metals and micronutrients, the level of pollutants appears to be not relevant for human health. Indeed, for example, the levels of Hg were in all areas much lower than those reported by European regulation (CE) N. 1881/2006 of the Commission of 19th December 2006 for safety from consumption of seafood. Also, As levels were very low, especially if compared with those of highly polluted areas as some in the Tyrrhenian Sea.

2.2 - Introduction

The pollution of the marine environment is a global concern because it concerns all water masses in the world and it is continuously increasing due to human activities that continuously produce and release contaminants into the environment through wastewater effluent discharges (Jones *et al*., 2004; Tornero and Hanke, 2017; Gharred *et al*., 2015). These contaminants such as pharmaceuticals, chemicals, pesticides, nanomaterials and xenobiotics can cause toxic effects to the health of marine organisms and indirectly to the health of humans who eat them (Axiak and Saliba, 1981; Tornero and Hanke, 2017). The Water Framework Directive (WFD, 2000/60/EC) provides for measures against chemical pollution of surface waters. Unfortunately, the environmental safety information for many chemicals in use today is seldom available, in particular as concern aquaculture and offshore industries. Furthermore, quantitative data on patterns of use and release of chemicals are also very difficult to obtain. Marine organisms, including fish, mollusks and echinoderms, accumulate pollutants such as heavy metals and hydrocarbons from the environment (Scanu *et al*., 2015). These inorganic and organic compounds (known as xenobiotic), stress communities and ecosystems by

interacting with the organism' physiology. As shallow waters are usually heavily and directly impacted by these pollutants, marine organisms of shallow coastal waters have a good potential to be used as bioindicators, hence providing early warning in coastal habitat under stress caused by the different types of pollutants. The aim of this research is to evaluate and compare different contaminant levels between urbanized and non-urbanized areas along the eastern coast of Sicily.

2.3 - Materials and methods

2.3.1 - Sampling area

The study was conducted in three different sites of eastern coast of Sicily: Ganzirri Lake (S1: 38°14'0.66''N, 15°50'8.90''E), is located near Messina city, its surface extends up to 0.338 km^2. Its maximum depth is 6.5 m with an estimated volume of $0.975x10^6$ l. The Lake receive a considerable amount of freshwater from the land. Hence, chemical-physical parameters are susceptible to high fluctuations (Giordani *et al.*, 2005). The second site is Ognina of Catania (S2: 37°53'0.66''N, 15°11'4.08''E), a small area located within the larger area of the Gulf of Catania. This area is characterized by the presence of mixed and rocky bottoms, close to the port of the city. The third area is the Natural Reserve of Vendicari (S3: 36°79'0.16''N, 15°09'5.12''E), south to Siracuse (SR). In this area bottom nature is characterized by the presence of seagrasses and mixed bottoms (sand and rocks). With the exception of the S3 (N.R. of Vendicari), all areas are located near large commercial port and highly urbanized area.

Fig. 17. Sampling areas in the oriental coast of Sicily (Google Earth).

2.3.2 - Sample collection and processing

A total of 20 specimens of sea urchin (*P. lividus*) were collected for each study area where they were caught randomly by local fishermen (only a Vendicari with authorization) in the period from May to June 2021. All specimens were transported in sea water coolers from the collection site to the laboratory of the University of Catania.

In the laboratory, the sea urchin test diameter (without spines) of each specimen was measured by electronic calliper (0.01mm precision). The test of each animal was opened with thin and pointed scissors, cutting from the peristomial membrane; the oral surface was carefully removed and then the gonads and the intestine of each specimen were removed with plastic tool for doesn't compromise the heavy metal analysis.

2.3.3 - Histological analysis

One gonad from each specimen were fixed in a 4% formalin solution for 24-48 h at 4°C. Subsequently, gonadal tissues were dehydrated using a scale of ethanol (from 35 to 100%), after in xylene for ultra-dehydration and finally included in paraffin. The blocks were cooled for approximately 15 minutes to speed up the paraffin solidification process and subsequently, were cutting sections of 5 μm and 3 μm by using a microtome. A total of 20 sections were obtained for each gonad, divided as follows: 5 for hematoxylin-eosin (HE) staining and 12 for immunohistochemical stainings, 3 duplicates for each antibody (MTs and HSP70) and 3 duplicates for respectively controls. After deparaffinization in xylene for 24 h and rehydration, the sections were stained whit respective protocols and the slides were mounted with a glass and coverslip by mounting medium (Entellant). For haematoxylin and eosin (HE) staining were used the protocol in according to Byrne (1990), Fabbrocini and D'Adamo (2010).

The gonad slides were observed and photographed under an optical microscope equipped with a digital camera; gonads are made of two distinct cell types: reproductive and storage cells. Thought the observation the size of female reproductive cells (oocytes) and the size of the follicle in males, compared to the thickness of the layers of storage cells, it is possible to identify the gametogenesis and the stage of maturation of each individual according to the classification developed for this species by several investigators (Byrne, 1990; Fabbrocini and D'Adamo 2010; Ouchene *et al*., 2021).

The reproductive stage of each animal was determined for each as follow:

- Stage I, recovery (gonad restoration): almost empty gonadal acini contain relict unspawned gametes.
- Stage II, growing: cleaning processes with participation of accessory cells and coelomocytes take place in gonadal acini to remove relict gametes.
- stage III, premature: developing activity, increase in the number of sex cells in the acini.
- stage IV, mature (active gametogenesis): growth and differentiation of sex cells.
- stage V, partly spawned: gonad is partially mature.
- stage VI, spent (postspawning): gonad is fully mature.

The slides were observed under an optical microscope (NIKON E200) equipped with a camera. Subsequently, to confirm the determination of the maturity stage, image analysis was performed using the open-access software ImageJ (as describe follow: 4.3.6 - Image analysis with ImageJ).

2.3.4 - Assessment of gonad state

The sex of sea urchins was examined by the macroscopic examination or with a slide examination, and the sex-ratio (♂/♀) was assessed using the following equation (Vafidis *et al*., 2019; Ouchene *et al*., 2021):

$$\text{Sex} - \text{ratio} = \frac{\text{N. of males}}{\text{N. of females}}$$

All specimen and all their gonads were weighed using a digital balance (0.0001 g precision). The Gonadosomatic Index (GI) is used to determine the reproductive state of *P. lividus* and it was calculated using the following equation (Carboni *et al*., 2015; Santos *et al*., 2019; Santos *et al*., 2020b):

$$\text{GI} = \frac{\text{gonad wet weight (g)}}{\text{total wet weight (g)}} \times 100$$

Gonad state of sea urchins was assessed based on semiquantitative indices. Gonad maturity stages were ranked as described previously (according to the classification), and the Gonad Maturity Index

(GMI) was calculated for female and male sea urchins using the following equation (Vaschenko *et al*., 2012):

$$\mathrm{GMI} = \frac{\sum(n \times F)}{N}$$

where $n =$ number of individuals in stage F, $F =$ stage of gonad maturity, $N =$ total number of individuals in the sample.

2.3.5 - Heavy metal analysis

Heavy metal analysis was carried out in collaboration with the Department of Medical, Surgical and Advanced Technologies "G.F. Ingrassia" of the University of Catania. Aliquots of sea urchin gonads were weighed using an analytical balance (0.0001 g precision) and then mineralized in a microwave oven (Ethos, TC, Milestone) equipped with Teflon vessels with 8 ml of 65% high-purity nitric acid (HNO3; Carlo Erba, Italy) for 50 minutes at 90°C. After acid digestion, the contents of the vessels were transferred to Falcon tubes and up to 50 ml of double distilled water (Merck, USA) was added to the samples. From each digested sample, 10 ml was filtered (0.22 µm filters) and taken for analysis and 50 µg/l of internal standard (Yttrium, Y, and Rhenium, Re, 1000 mg/l Merck, USA) was added as an internal quality control. Quantification of trace elements and micronutrients was performed using an Inductively Coupled Plasma - Mass Spectrometer (ICP-MS) Elan-DRC-e (Perkin Elmer, USA).

Concentrations were determined using standard solutions prepared in the same reagent matrix. Standards for instrument calibration were prepared based on certified monoelement reference solutions ICP Standard (Merck, USA). For quality control, one sample for each batch of mineralization was processed in duplicates; one was spiked with a multi-element solution of 25 mg/l at 5 mg/kg and we obtained a mean recovery of 85.2-105% for all trace elements and micronutrients. The method detection limit (MDL) was calculated based on the 40 CFR 136, EPA procedure for digested analytical blanks using the following equation:

MDL = t (df = n-1, p= 0.99%) × SD,

where t represents the one-tailed Student's t distribution, df represents the degrees of freedom, n represents the number of blank replicates, p represents the probability, and SD represents the standard deviation. Levels of the following contaminants and elements were measured in the gonads of the species: As (Arsenic), Cd (Cadmium), Co (Cobalt), Cr (Chromium), Cu (Copper), Hg (Mercury), Mn

(Manganese), Ni (Nickel), Pb (Lead), Se (Selenium), V (Vanadium) and Zn (Zinc). LOD mg/kg wet weight (w.w.) calculated for the metals/metalloids analysed are the following: As (0.052), Cd (0.014), Co (0.062), Cr (0.046), Cu (0.264), Hg (0.009), Mn (0.101), Ni (0.062), Pb (0.010), Se (0.070), V (0.053), and Zn (0.418). Of these, only for Hg, Cd and Pb there are maximum level indication for human health following the European regulation (CE) N. 1881/2006 of the Commission of 19th December 2006.

Echinoderms are not included in the list. Hence, using a precautionary approach, we considered the highest levels reported for bivalves as reference points: for Hg, Cd and Pb considering the maximum acceptable level respectively 0.5, 1.0 and 1.5 mg/Kg.

2.3.6 - Immunohistochemical analysis

According to Pecoraro *et al*. (2018) the immunofluorescence protocol was performed and modified for gonad slides to detect positivity to the biomarkers MTs and HSP70. After 24-48 h in xylene for the deparaffinization, the slides were hydrated in decreasing alcoholic solutions (from 100 to 35%) and washed in distilled water for 2 minutes in vertical position. Subsequently they were placed horizontally in a humid chamber, covered with Methanol + H_2O_2 (9:1 ml) solution for 15 minutes and washed in PBS buffer (pH 7.4, 0.1 M) 3 times for 3 minutes each. Then the slides were incubated for 20 minutes in 1% BSA, blocking solution to fill non-specific binding sites of the antibodies and were incubated overnight in a humid chamber at 4°C with the primary antibodies: anti-mouse-MTs and anti-rabbit-HSP70 (GeneTex, 1:1000); no primary antibody was used for the control slides. After rinsing in PBS buffer (pH 7.4, 0.1 M) 3 times for 3 minutes, the samples were incubated for 1 h at 4°C in the dark with FITC-conjugated anti-mouse secondary antibody for MTs and TRITC-conjugated anti-rabbit secondary antibody for HSP70 (GeneTex, 1:1000); the first show green fluorescence and the second in red. Subsequently the slides were washed again in PBS (3 times for 3 minutes), dehydrated in increasing alcoholic solutions (From 70 to 100%) for 2 minutes each and dried in air in the dark. Finally, the slides were mounted with Fluoromount G with DAPI (Invitrogen) for blue fluorescence nuclear dye. Observations were made with the NIKON ECLIPSE Ci fluorescence microscope and images acquired with the NIKON DS-Qi2 camera.

2.3.7 - ImageJ analysis

Through ImageJ software (Kainz *et al.*, 2015) it was possible to evaluate the gonadal stage by observer-independent method; HE stains makes a difference in the colour pattern between gametogenic cells and non-germinal accessory cells; the firsts are basophilic and show violet colour, while the rest are eosinophilic and show pink colour (Byrne, 1990). This new approach described by Mantilla *et al*. (2020) takes advantage of image analysis to assess in histological preparations of the gonads the cellular growth of germ cells and calculate a Pixelar index (PI). The PI can be calculated considering just the proportion of the area covered by germinal vs somatic cells in the gonad follicle (PI_1) or computing also the empty space created in the follicle lumen after spawning (PI_2), which reduces the variability of the index (Mantilla *et al*., 2020).

Briefly, a total of 10 photographs taken of the gonad slides stained with HE of sea urchins from each sampling area were analysed, through ImageJ using the Colour Deconvolution plugin (v.3.0.2 Fiji software). This tool allows us to obtain the violet and pink layers of HE stains obtained from 10 specimens of each study area; these were transformed in a binary format of black and white. The cleaned images were transformed to grey scale, the background was changed to black, and finally the images were transformed to binary format to evaluate the white pixels of the original photograph. The black pixels coming from the violet layer represent only germinal cells by follicle, from pink layer represent other cellular populations (nutritive phagocytes NPs and non-germinal accessory cells) and coming from grey scale pictures in binary format represent the lumen of the follicle. This pixel information was used to calculate two indices, termed Pixelar index (PI): the first (PI_1) represent the ratio between the violet pixels in relation to violet plus pink is computed, while in the second (PI_2), white pixels (empty space or lumen) are also considered (Mantilla *et al*., 2020).

Moreover, ImageJ software (Bankhead, 2014; Wiesmann *et al*., 2015) has been used to process the images obtained by fluorescence microscope since it calculates the mean value (the sum of the values at all pixels divided by the number of pixels) of a defined area using the split channel mode (blue, red and green) respectively for the wavelength of the antibody. For each photo, the same area (macro) was analysed to obtain density histograms.

2.3.8 - Statistical analysis

Statistical data was analysed using GraphPad Prism software (version 9.3.1) and the same software was used to create the graphs and tables. Sex-ratios were tested against a 1:1 ratio with chi-squared test for determinate the difference between males and females ($p<0.05$). For Gonad Index (GI) and the semi-quantitative Index of Gonads Maturity (GMI) the data were expressed as mean and standard deviations (±SD) and were analysed with two-way ANOVA followed by Tukey's hoc test for difference between groups (males and females and per sampling sites) ($p <0.05$).
For all immunohistochemicals images the mean value (the sum of the values at all pixels divided by the number of pixels) of all selected area was calculated. For each photo, the same area (with setting a macro for acinals) was analysed in order to obtain density histograms. The mean values were compared with GraphPad Software by t-student test to detect significant differences between the photos of immunohistochemical slides and photos of control groups ($p < 0.05$).
The data obtained from heavy metals analysis were analysed by one-way ANOVA, followed by Tukey's post hoc test for differences between elements and their means in each sampling sites. The level of significance was set at $p<0.05$. All data are represented as mean and standard deviation (± SD). Statistically significant data are indicated with a symbol (*$p<0.05$ and **$p<0.01$).

2.4 - Results and discussions

2.4.1 - Assessment of gonad state

In total, 60 *P. lividus* specimens were processed, 20 for each sampling area: the mean size of tests was 46.60 ± 4.24 mm at S1, 45.50 ± 4.72 mm at S2 and 52.10 ± 2.77 mm at S3. The sex ratio was significantly biased in favour of females in stations S2 (1:0.33; p-value=0.02) and S3 (1:0.25; p-values=0.007). These results are in agreement with those reported in literature from some areas of the western and southern Mediterranean Sea (Vafidis *et al*., 2019).

Females of S3 station showed the highest values of GI (4.61 ± 1.39), while the lowest value of GI was obtained for females of S2 (1.89 ± 0.67) and a mean value of GI of 3.43 ± 1.43 for females of S1 station (Tab. 2). No statistical difference was recorded between GI values between sexes, while a clear statistical difference was recorded between the values of GI at different locations (p-value<0.01), and in particular between S1-S2 and S2-S3 (Fig. 18).

SITE	SEX		SEX RATIO (♂/♀)		GI (%)
S1 (ME)	Females ♀	12	1 : 0.67	60 (♀\%)	3.43 ± 1.43
	Males ♂	8		40 (♂\%)	3.80 ± 1.67
S2 (CT)	Females ♀	15	1 : 0.33	75 (♀\%)	1.89 ± 0.67
	Males ♂	5		25 (♂\%)	2.30 ± 0.35
S3 (SR)	Females ♀	16	1 : 0.25	80 (♀\%)	4.61 ± 1.39
	Males ♂	4		20 (♂\%)	3.62 ± 1.10

Tab. 2. Sex ratio and percentages of GI of *P. lividus* gonads for all sampling areas.

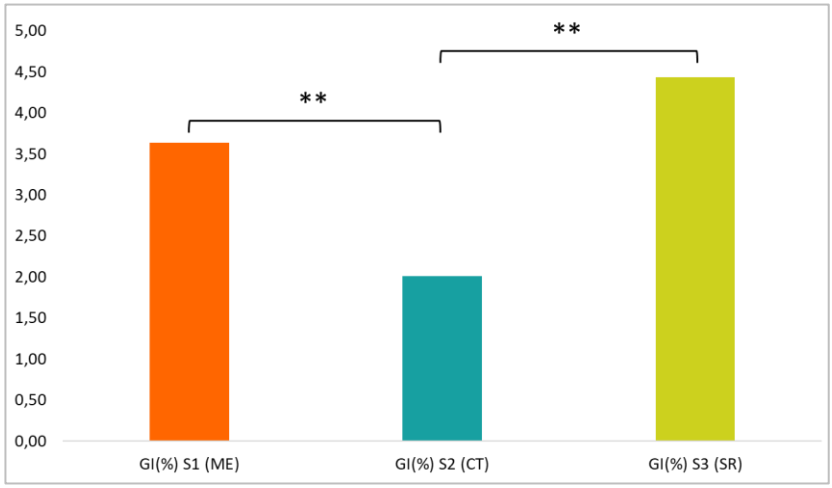

Fig. 18. Comparison of GI percentages of different sampling areas (**p<0.001).

Obtained values of GI are in agreement with those reported in literature for the same period. The values of GI decrease gradually from March to August, while increase from October to January-February, when they reach the peak along the southwestern coast of the Mediterranean Sea (Ouchene *et al*., 2021). From results, appear that *P. lividus* specimens collected in the S2 were less mature than those collected in S1 and S3.

Hystological analysis showed that *P. lividus* specimens from the different sampling stations were in different reproductive phases (Fig. 19). In general, we can state that specimens in S1 and S2 were in maturation or already mature (stage III and stage IV), while in S3 gonads were in advanced maturation stage (stage V and stage VI), with some specimens in recovering phase (I).

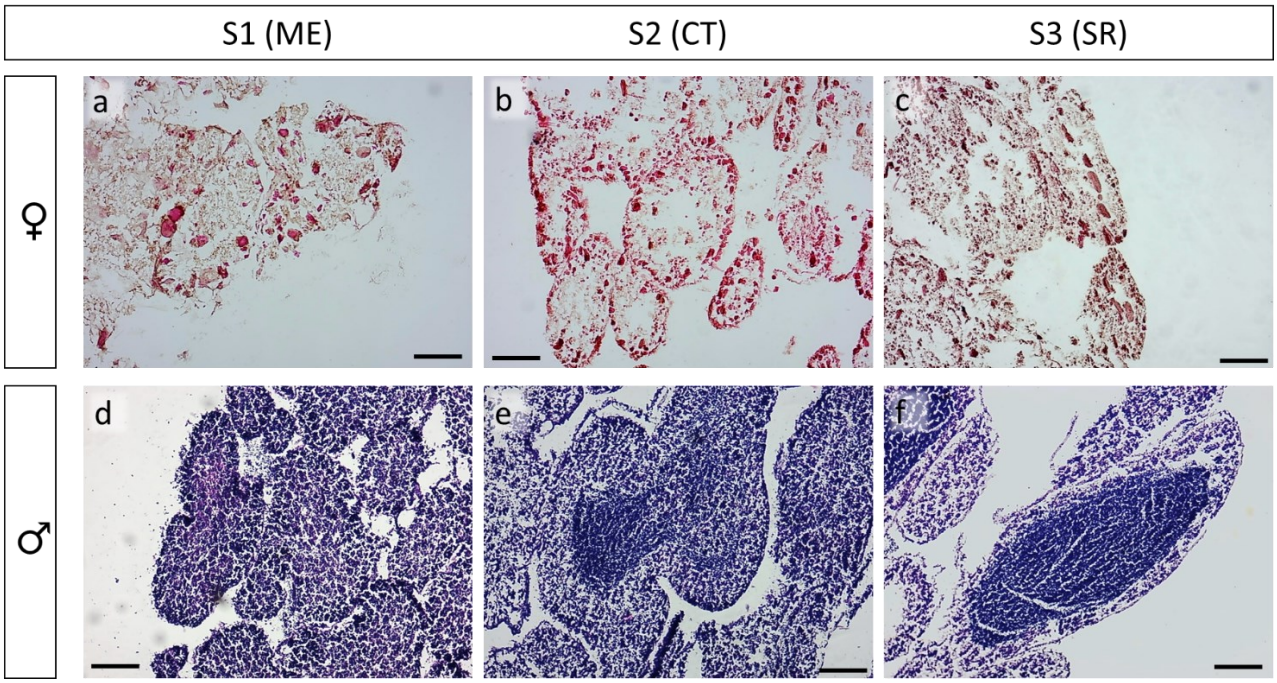

Fig. 19. Histology with HE stained of ovary and testes of *P.lividus* collected in the three sampling areas: a) female of S1 in III stage; b) female of S2 in III stage; c) female of S3 in VI stage; d) male of S1 in III stage; e) male of S3 in IV stage; f) male of S3 in VI stage. Scale bar =100 µm (by Sara Ignoto with NIKON E200).

In particular, for station S1 were recorded specimen from II to IV maturity stage with a greater frequency (50%) at III maturation stage for females and at 50% at IV stage for males. In two female specimens, they were observed histopathology. These specimens showed atretic oocytes and several nutritive phagocytes (NPs) in all gonad areas and 3 male specimens with several hypertrofic NPs in lumen and peripheral gonad area, within which they were present abundant globular inclusions Lipofuscin-Like Pigment (LLP) as showed in literature (Vaschenko *et al*., 2012) (Fig. 20a,b). However, due to the low number of samples, no further investigations were conducted on this aspect.

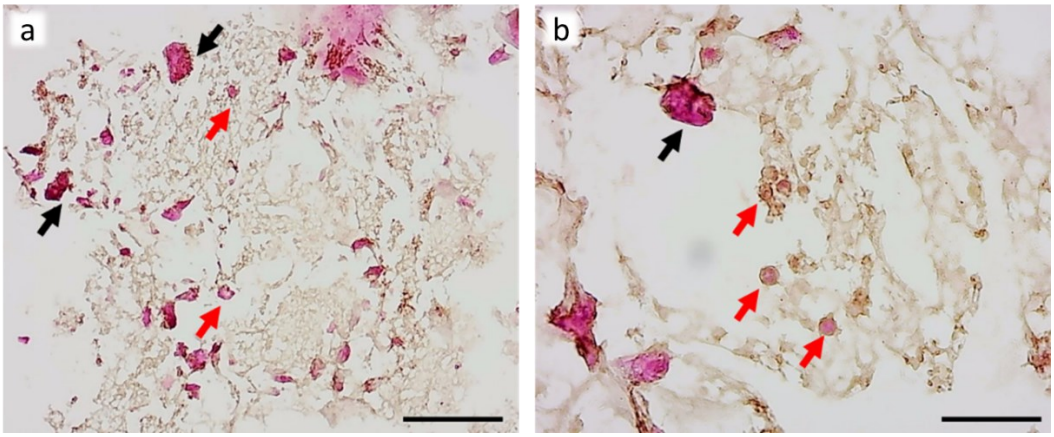

Fig. 20. Examples of histopathologies in female gonad of S1 *P. lividus*; a) female with atretic oocytes (black arrow) and hypertrophic NPs (red arrow). Scale bar = 150 µm; b) female with atretic oocytes (black arrow) and hypertrophic Nps (red arrow). Scale bar = 250 µm (by Sara Ignoto with NIKON E200).

For the S2 the most common maturity stages were III and IV; 53% at III for females and 40% at II and III stages for males. In this station also in both sexes were found numerous NPs, but of normal size. Despite differences recorded for GI values the maturation stages between S1 and S2 were similar. Gonadal index, however, is not a direct measure of the gametogenic status and no clear relationship between gonadal index and reproductive stage has been established, this method is therefore to be considered with caution. Indeed, this index is based on gonad weight that can varies depending on nutrition state and environmental conditions. For these reasons in literature, they were recorded results in disagreement (Carboni *et al*., 2014).

For the station S3, the most common stages were from V to I, with the highest frequency of VI (50%) for both sexes. This sampling area was the only one of the three areas examined which showed mature individuals in accordance with the widely described reproductive cycle of *P. lividus*. This could be attributed to the fact that S3 is a Natural Reserve, therefore less subject to fishing pressures and to all those favorable environmental conditions that a MPA can guarantee (Marcos *et al*., 2021).

In all cases, no statistical differences were found in GMI values between sexes and sampling sites (Tab. 3). From image analysis with ImageJ, they were calculated the mean values of the following Pixelar Indices (PI_1 and PI_2), showed in Tab. 3. These indices respectively indicate the relationship between purple pixel (germinal cells) and pink pixel (accessorial non-germinal cells) in the gonad follicle, considering with the second index also the lumen ("empty space") of analyzed follicles.

SITE	SEX	N. Stage of Reproductive cycle						GMI	PI_1 (%)	PI_2 (%)
		I	II	III	IV	V	VI			
S1 (ME)	F ♀ (12)	0	1 (8%)	6 (50%)	5(42%)	0	0	3.33	15.80 ± 1.51	21.83 ± 1.25
	M ♂ (8)	0	1 (13%)	3 (38%)	4 (50%)	0	0	3.38	18.37 ± 1.34	20.62 ± 1.44
S2 (CT)	F ♀ (15)	0	3 (20%)	8 (53%)	4 (27%)	0	0	3.07	20.26 ± 0.95	27.04 ± 1.58
	M ♂ (5)	0	2 (40%)	2(40%)	1 (20%)	0	0	3.20	19.58 ± 1.27	22.12 ± 2.14
S3 (SR)	F ♀ (16)	6 (38%)	0	0	0	2 (13%)	8 (50%)	4.27	22.96 ± 2.01	30.06 ± 1.53
	M ♂ (4)	0	0	0	0	2 (50%)	2 (50%)	5.50	23.30 ± 1.32	24.11 ± 1.67

Tab. 3. Summary table of the stages of maturity observed and the values of GMI and Pixelar index obtained for all sampling areas.

The values obtained with this analysis are in agreement with those obtained with GMI analysis, further supporting the presence of different maturation stages in the three sampling stations, with the exception of the S1 that showed lower levels of PI_1 and PI_2 for both sexes (Fig. 21). No statistical differences were found between sampling stations.

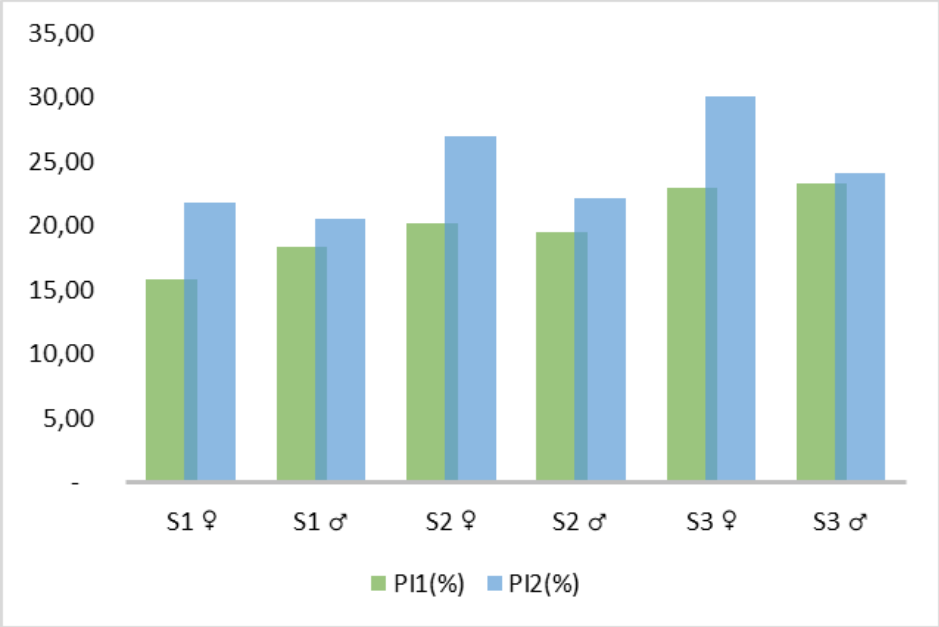

Fig. 21. Comparison of PI_1 and PI_2 obtained for all sampling areas

2.4.2 - Heavy metal analysis

Data obtained from analysis of elements, were divided in contaminants (As, Cd, Hg and Pb) and micronutrients (Co, Cr, Cu, Ni, Se, V, Zn and Mn). Analysis results clearly showed as the Arsenic (As) was the most abundant contaminant in gonads of sea urchin in all sampling stations (Fig. 22). In particular, S3 showed the highest values of this contaminant. These results are statistically significative if compared with those of S2: 4.45±2.18 mg/kg vs. 2.45±0.77 mg/kg, respectively.

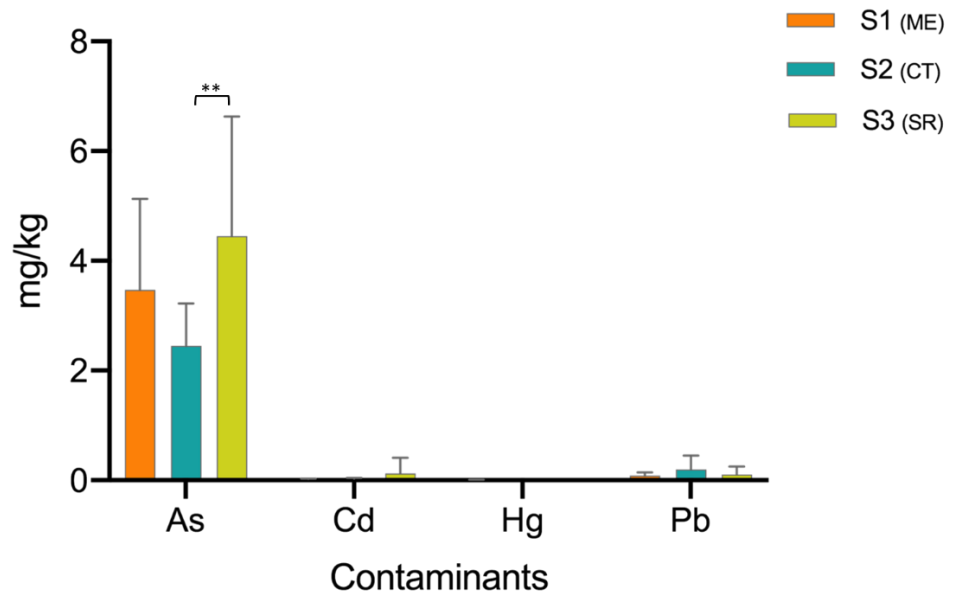

Fig. 22. All contaminant analysed in *P. lividus* gonads for each sampling areas (**p<0.001).

Levels of Hg (mercury) was very low (Fig. 23), in specimens of S1 was 0.014±0.003 mg/kg. This value is significantly lower than maximum level indicated for human health by the European regulation (CE) N. 1881/2006 of the Commission of 19th December 2006, (0.5 mg/kg for Hg).

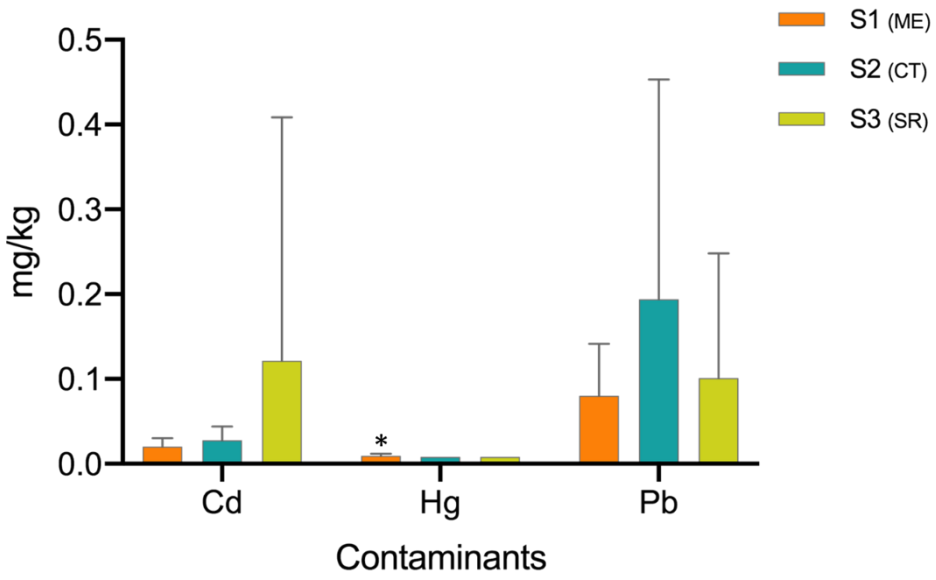

Fig. 23. Contaminants in the gonads of *P. lividus* (without As) (*p<0.05).

Concerning micronutrients' analysis, Zn reached the highest values in all stations (Fig. 24), showing the following values for S1, S2 and S3 respectively: 21.98±24.44 mg/kg, 16.73±13.97 mg/kg and 21.26±18.61 mg/kg. No statistical difference was obtained between the values in the different stations.

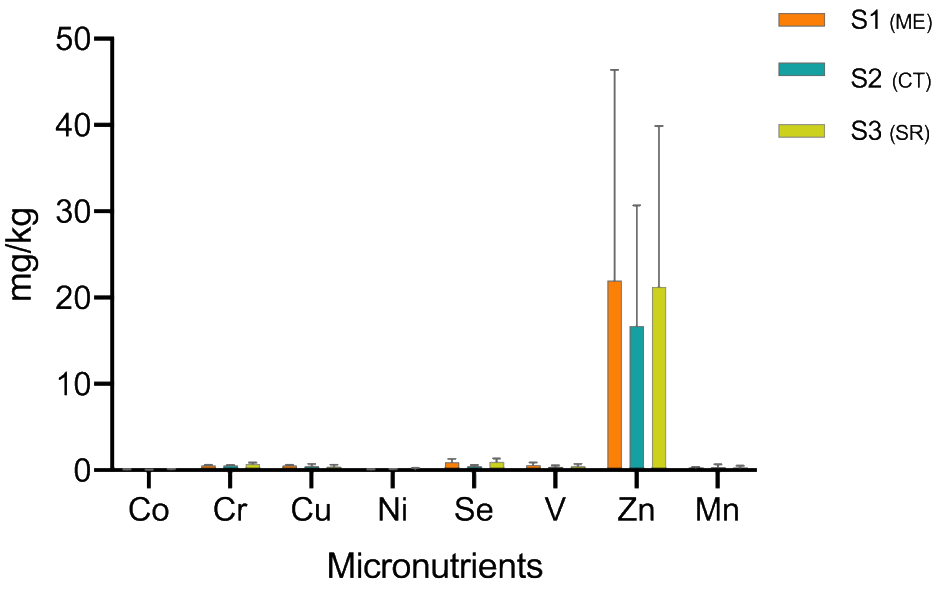

Fig. 24. All micronutrients analysed in the gonads of *P. lividus* for sampling areas.

Values of Co, Cr, Ni, Se and V were statistically different depending on the area ($p < 0.01$). The most elevated mean values were recorded for Cr, in which were reported statistically different values between S1-S3 and S2-S3. For Se significant differences were recorded for S1-S2 and S2-S3. For V statistical difference were recorded for the comparison S1-S2 ($p < 0.05$).

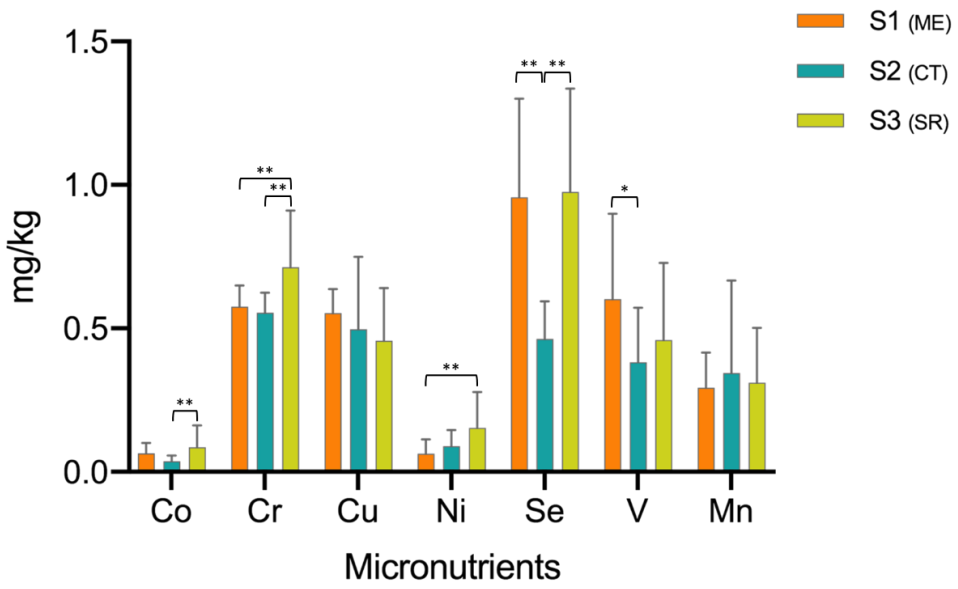

Fig. 25. Micronutrients present in the gonads of *P. lividus* for all sampling areas (without Zn) (*p<0.05; **p<0.001)

Furthermore, from analysis emerged also a statistically relevant difference between contaminants and microelements values in both sexes (gonads) (Tab. 4). In particular, as concern S1, there was a

statistical difference between sexes for the following elements: As, Cd, Se and Zn. For S2 only Zn showed relevant differences between sexes, while for S3 only As and V.

S1 (ME)			
Elements	P value	Mean of Males (mg/kg)	Mean of Females (mg/kg)
As*	0,0418	2,5580	4,0760
Cd*	0,0187	0,0143	0,0243
Co	0,7750	0,0616	0,0665
Cr	0,7452	0,5689	0,5803
Cu	0,0829	0,5929	0,5261
Hg	0,0535	0,0106	0,0083
Mn	0,1818	0,2483	0,3236
Ni	0,6085	0,0558	0,0680
Pb	0,7282	0,0744	0,0844
Se*	0,0295	0,7566	1,0900
V	0,9120	0,5924	0,6080
Zn*	0,0154	6,4120	32,3600
S2 (CT)			
Elements	P value	Mean of Males (mg/kg)	Mean of Females (mg/kg)
As	0,7614	2,3560	2,4820
Cd	0,5401	0,0240	0,0292
Co	0,4010	0,0302	0,0393
Cr	0,0716	0,6030	0,5385
Cu	0,3633	0,5880	0,4658
Hg	1,0000	0,0080	0,0080
Mn	0,7660	0,3050	0,3567
Ni	0,9620	0,0900	0,0885
Pb	0,9882	0,1922	0,1943
Se	0,5366	0,4310	0,4742
V	0,8647	0,3682	0,3857
Zn*	0,0081	3,1910	21,2400
S3 (SR)			
Elements	p-values	Mean of Males (mg/kg)	Mean of Females (mg/kg)
As*	0,0367	6,4440	3,9540
Cd	0,0559	0,3643	0,0605
Co	0,0750	0,1463	0,0710
Cr	0,2592	0,8148	0,6877
Cu	0,0503	0,6158	0,4167
Hg	1,0000	0,0080	0,0080
Mn	0,6870	0,3465	0,3019
Ni	0,1299	0,2385	0,1318
Pb	0,5201	0,0570	0,1118
Se	0,0727	1,2640	0,9041
V*	0,0340	0,7088	0,3969
Zn	0,1984	10,3700	23,9900

Tab. 4. Results of t-test student for contaminants and micronutrients in female and in male of *P. lividus* for each sampling areas (*p<0.05).

As concern contaminants levels in gonads, As resulted to be the most relevant. However, recorded values are markedly lower than those reported from highly polluted areas, we As levels reaches values of di 164.1 mg/kg (Scanu *et al*., 2015). These high levels of As can be cause from both geological nature of the area and presence of industry that use hard coal. The other values recorded for other contaminants were very low and probably don't represent threats for human health.

As regard Zn, it was the most abundant micronutrients in gonads of sea urchin in all stations, especially in those of female specimens. This is in agreement with data reported in literature, both for different sea urchin species and geographical areas (Vashenko *et al*., 2012). Indeed, it is reported that values of this element are usually greater in female specimens because sex-specific differences in the metabolism of major yolk protein (MYP), a superfamily protein that transports Zn from the digestive tract to the ovary and testis through the coelomic fluid, because Zn is essential for gametogenesis (Unuma *et al*., 2007; Vashenko *et al*., 2012).

2.4.3 - Immunohistochemical analysis

The results of the immunohistochemical analysis confirm absence of positivity in the expression of both biomarkers (HSP70 and MTs), so there was not statistically significant difference to the gonad slides of all sampling area compared to the control slides.

As regard MTs, there was no positive biomarker response at all sampling areas even in both females and males (Fig. 26a,b).

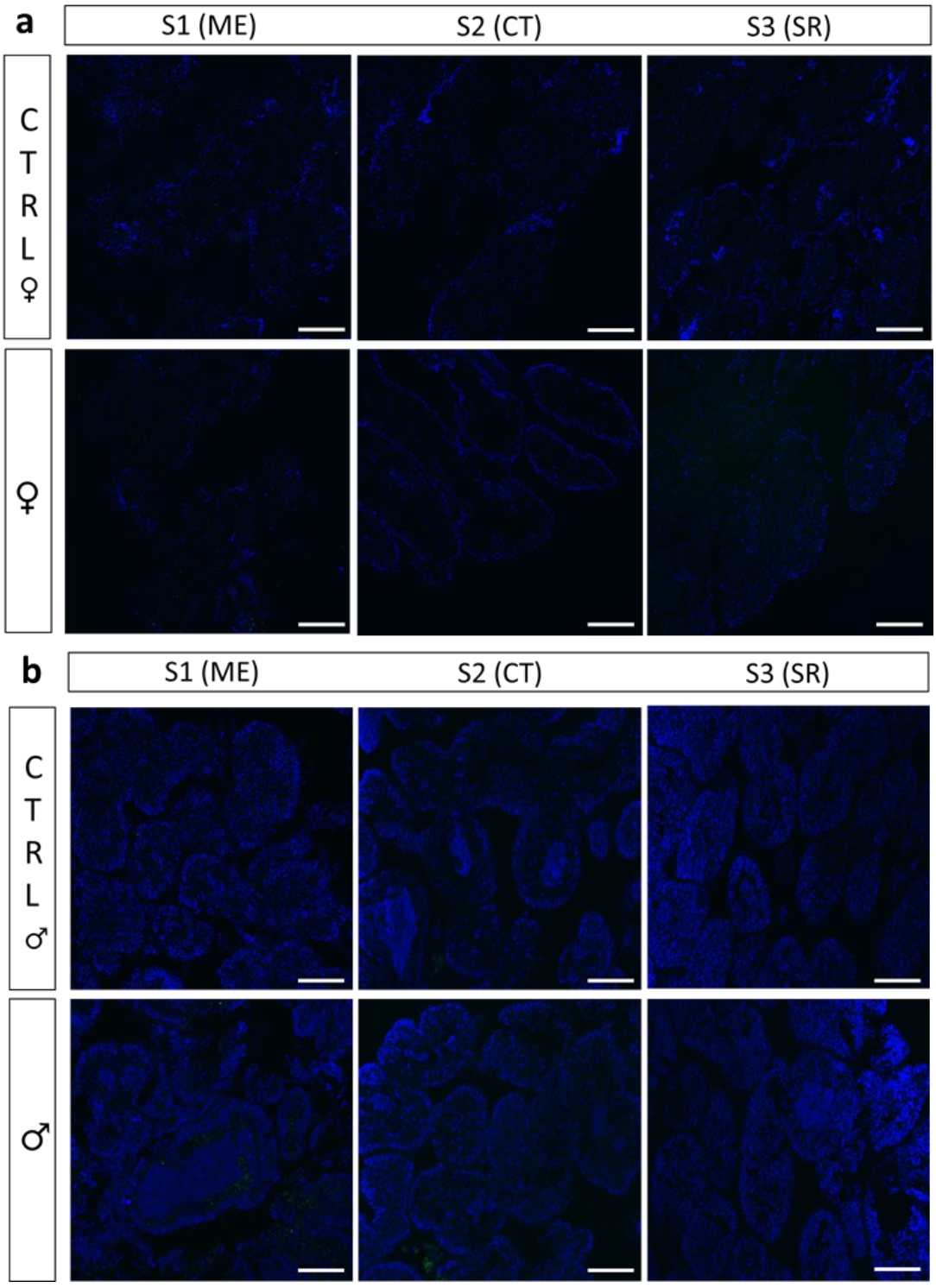

Fig. 26. Table of MTs antibody-staining of ovary and testes of *P. lividus* in all sampling areas: a) female and respectively controls slides (CTRL). Scale bar = 100 µm; b) male and respectively controls slides (CTRL group Mts). Scale bar = 100 µm) (by Sara Ignoto).

As regard HSP70, there was no positive biomarker response at all sampling areas even in both sexes (Fig. 27a,b).

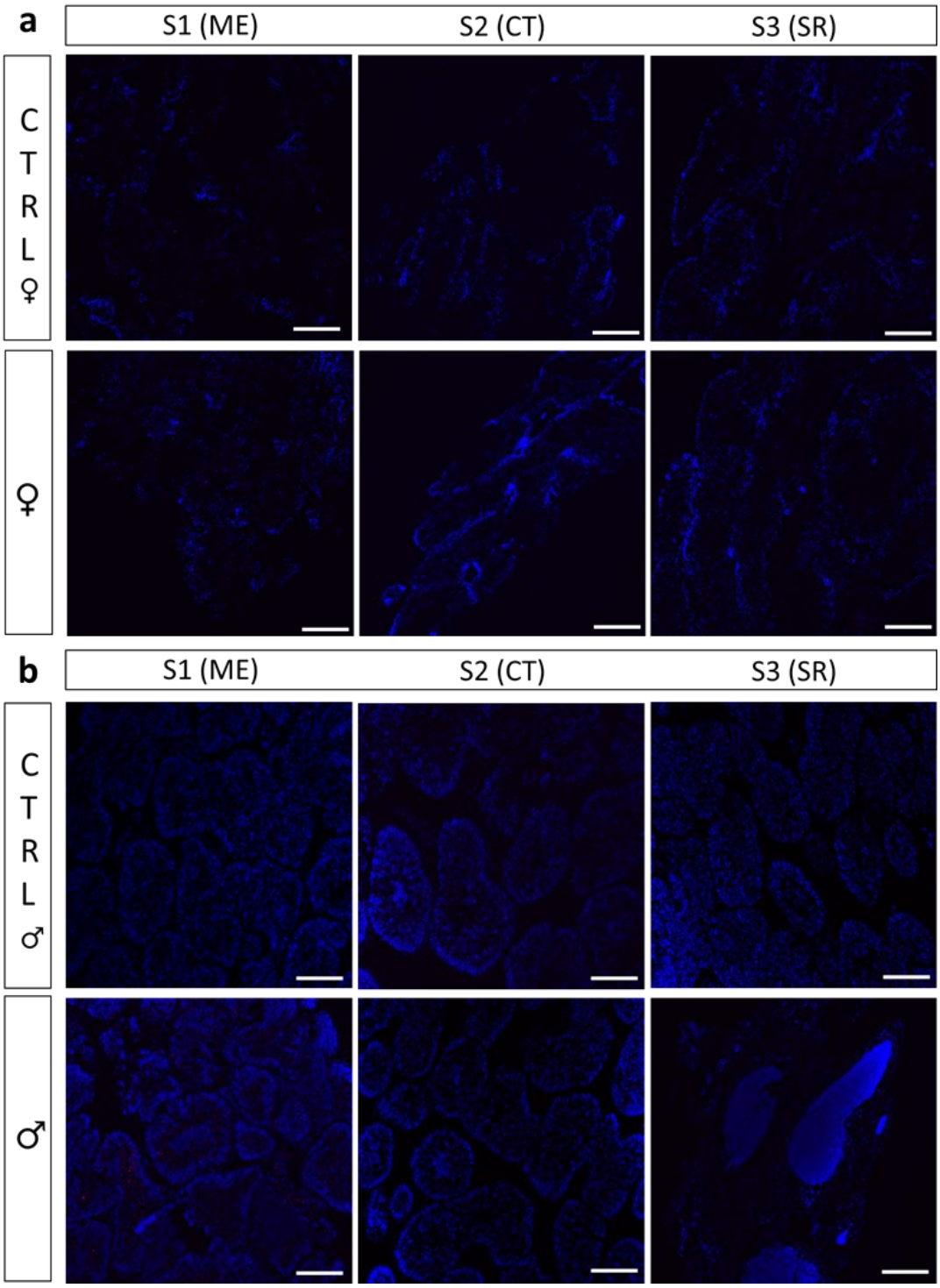

Fig. 27. Table of HSP70 antibody-staining of ovary and testes of *P. lividus* in all sampling areas: a) female and respectively controls slides (CTRL group HSP70). Scale bar = 100 µm; b) male and respectively controls slides (CTRL). Scale bar = 100 µm) (by Sara Ignoto).

In few samples taken in the S1 study area and in III stage of maturity, both for Mts and HSP70, the analysed images showed bright spots at the respective wavelengths (Fig. 28). These spots correspond to globular inclusions Lipofuscin-Like Pigment (LLP) that in *Strongylocentrotus intermedius* show a strong autofluorescence exhibited at excitation maximum of 450 nm and emission maximum of 512 nm (emission spectrum of autofluorescence from 460 to 600 nm) (Vaschenko *et al*., 2012).

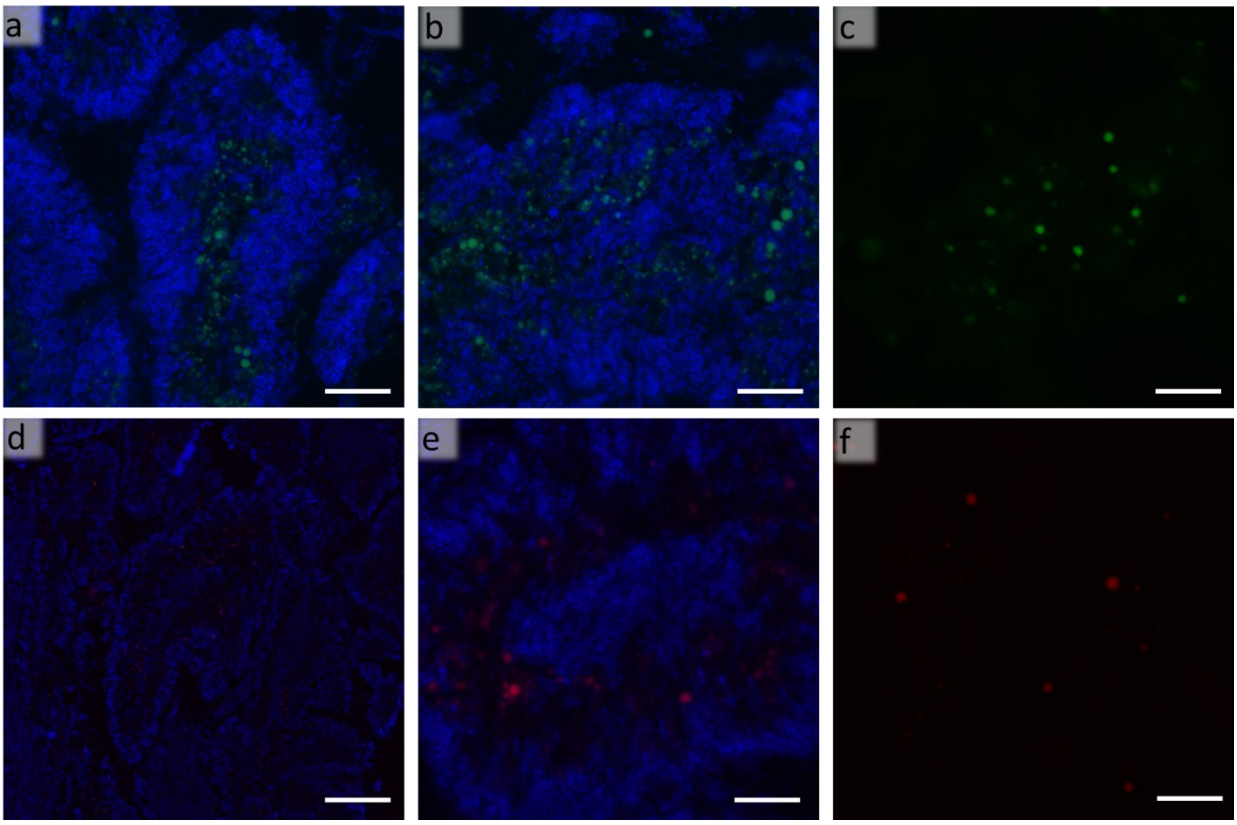

Fig. 28. LLP autofluorescence in *P. lividus* gonads of S1: a) male of CTRL group (MTs) in III stage of maturity. Scale bar = 100 µm; b) male MTs antibody-staining in IV stage. Scale bar = 200 µm; c) female of CTRL group (MTs) in IV stage). Scale bar = 200 µm; d) male of CTRL group (HSP70) in IV stage of maturity. Scale bar = 100 µm; e) male HSP 70 antibody-staining in IV stage. Scale bar = 200 µm; f) female of CTRL group (HSP70) in IV stage). Scale bar = 200 µm (by Sara Ignoto).

Given the wavelengths used in this study (Green 520-560 nm and Texas red 561-594 nm), it was possible to observe the presence of LLP also in gonad of *P. lividus* sampled in the S1 area (5 specimens) both controls stained and complete immunohistochemical stained. There are currently no data in the literature describing these lipopigments in this species. However, it is known that these LLP was accumulated in different compartment of gonads and into the cytoplasm of NPs or the cytoplasm of oocytes (Byrne, 1990; Schäfer *et al*., 2011; Arizza *et al*., 2013). NPs was mostly accumulated to the acinal periphery of the gonad during the gonadal growth and maturation phase

(Stage III) for phagocyte both relict gametes in postspawned gonad and abnormal sex cells in the developing gonad.

The most important functions of NPs are phagocytosis of relict and abnormal gametes, restoration of nutritive substances, and participation in nutrition of growing and differentiating gametes (Reunov *et al*., 2004; Walker *et al*., 2005). So, the presence of abundant and hypertrophic Nps in all compartments of the gonads may indicate the presence of histopathology.

In addition, in female sea urchins, a portion of MYP (a superfamily protein that transports Zn during gametogenesis) is transported from NPs to the ovary and finally forms yolk granules (Vaschenko *et al*., 2012). This might be a reason for Zn accumulation in sea urchin ovary of S1. However, Vaschenko and colleagues (2012) confirm that the quantity of LLP content in sea urchin NPs can not be used as a biomarker in marine pollution monitoring.

2.5 - Conclusion

Marine pollutants can have deleterious effects on marine ecosystem and indirectly affect human health. Marine organisms, including echinoderms, accumulate pollutants such as heavy metals and hydrocarbons from the environment and have a good potential to be used as biomarkers, hence providing early warning in coastal habitat under stress caused by pollution. From results obtained for the different maturity indices (GI, GMI and Pixelar Index) is clear that sea urchins collected in S3 are in advanced stage of maturity, with most common presence of VI and I (post-spawing) unlike sea urchins sampled in S1 and S2 with different specimens at III and IV stages. In literature, the presence of two reproductive peak was reported for *P. lividus* during the year: March-April and November-December. However, in Italian waters the first reproductive peak can extend to May-June. This is in agreement with what we found in S3. On the other hand, it was expected to found sea urchins in S1 and S2 in a more advanced maturation stage. This could be due to different factors, such as fishing pressure, chemical-physical parameters of waters and marine pollution. Further studies are necessary to better understand these aspects; furthemore, several researchers suggested a substantial revision on the fishing rest of the species (Vafidis *et al*., 2012).

However, considering the values obtained for contaminants analysed in *P. lividus* gonads in these sampling areas and from comparisons with literature and legal references, it was possible state that the overall contaminant levels was low, even if, as reported in literature, their levels can be dependent from sampling periods (Rouane-Hacene *et al*., 2018). Arsenic levels were different depending on the

sampling station, however, values obtained were quite low, especially if compared with those of other areas (Tyrrhenian Sea) that are highly contaminated by this pollutant. As regards micronutrients levels, the high level of Zn recorded in gonads of sea urchins sampled in S1 (premature) and S3 (postspawning). This could be related to the maturation stage, because Zn concentrations are positively correlated with gonadic maturation. From histological analysis, a pathology was recorded in some specimens collected in S1, but it was not possible to draw conclusions because the low number of specimens analyzed. Further detailed studies are necessary in order to better observe and quantify different types of histopathology and correlate them with heavy metals concentrations in the investigated areas, especially in S1.

CHAPTER 3 - *PARACENTROTUS LIVIDUS* AS A MODEL ORGANISM FOR NANOMATERIAL APPLICATIONS

3.1 - Abstract: evaluation of spermiotoxicity in *P. lividus* by nano-TiO_2 compounds applied to water remediation

A lot of pollutants reach directly or indirectly the aquatic environments. Depending on the nature of such contaminants, they can negatively impact on aquatic ecosystems (Piwowarska and kiedrzynska, 2021). In this context, water remediation can represent a valid solution to reduce the impacts of xenobiotics that reach the marine environment through wastewaters (De Oliveira *et al*., 2020). Among the most popular remediation method, nanomaterials cover an increasing importance and utilization in order to counter water pollution (Ahmed *et al*., 2021). However, despite their great utility in do this, the effects of nanoparticles on marine systems are unknown and unpredictable (Timerbaev *et al.*, 2021). Therefore, it becomes necessary to test these nanomaterials to assess the presence of potential negative effects on aquatic life. Some studies have evaluated the toxicity of the most common nanoparticles such as ZnO, Ag and TiO_2 on spermatozoa, larvae and adults of the sea urchin *Paracentrotus lividus* (Lamarck, 1816), generally demonstrating toxic effects that dramatically affect the survival rate of embryos (Gambardella *et al*., 2013; Manzo *et al*., 2013, 2017). In particular, TiO_2 sol-gel type and TiO_2-rGO, nanocomposites with graphenic structures, are the most promising materials for enhancing the photocatalytic activity (Macwan *et al*., 2011; Balsamo *et al*., 2021). The aim of this study was to evaluate the effects of TiO_2 sol-gel and TiO_2-rGO nanocomposites on both viability and motility of spermatozoa of *P. lividus*. The spermatozoa were exposed at different times (30, 60 minutes) and concentrations (10, 20, 40 μg/ml) of both nano-TiO_2 nanocomposites. The results clearly showed a decrease in both viability and motility of *P. lividus* spermatozoa exposed to TiO_2 sol-gel and TiO_2-rGO nanoparticles. In particular, viability and motility resulted to be inversely related to both exposure time and concentration of TiO_2 sol-gel and TiO_2-rGO nanocomposites than control group. In conclusion, although nanomaterials represent a new generation of technologies involved in water purification, their release in aquatic ecosystems can potentially endanger aquatic life. Hence, the urgent need to further investigate and test the potential risks of this materials through both extensive laboratory and field studies.

3.2 - Introduction

Emerging contaminants, discovered in the 19th century, have entered the environment at a worrying rate, but have only recently been identified as major water pollutants (De Oliveira *et al*., 2020). This definition includes highly polar and acidic/alkaline compounds (Rego *et al*., 2021) such as pharmaceuticals and personal care products, hormones, dioxins, pesticides, surfactants, polycyclic aromatic hydrocarbons, alkylphenolic compounds, nanomaterials and fluorinated substances (Naidu *et al*., 2016; Tijan *et al*., 2016; Ahmed *et al*., 2021). One of the risks related to emerging contaminants is that they can bioaccumulate in lipid-rich tissues of organisms due to their hydrophobic properties and cause damage to the endocrine systems of humans and animals and spread antimicrobial resistance (Rodriguez-Narvaez *et al*., 2017); in general, they can influence the growth, reproduction and evolution of species in the environment.

There are many methods used to remove emerging contaminants from water, and among these the photocatalysis, which requires the use of catalysts to facilitate the transfer of energy from the photon to a water molecule, is one of the most used. Photocatalysis using TiO_2 as a catalyst in recent decades has proven useful for removing pollutants and microorganisms from wastewater. TiO_2 is a versatile compound found in nature in the forms of rutile, anastase and brookite. It is considered an ideal semiconductor for photocatalysis especially in the form of nanoparticles and is one of the most frequent catalytic methods used in water remediation (Gupta *et al*., 2010).

The advantages of this advanced oxidation treatment are reduced costs, flexibility in the reuse of the catalyst, operation at environmental temperature and pressure, the possibility of using sunlight to irradiate the catalyst and also guarantees the complete mineralization of aliphatic organic pollutants, aromatics, polymers, dyes, surfactants, pesticides and herbicides in CO_2, water, mineral acids (Ahmed *et al*., 2021). However, there are some disadvantages, including the difficulty in obtaining uniform radiation over the entire catalyst surface on a larger scale; the ability to absorb only UV light, and the rapid recombination of the charge which decreases its photocatalytic activity (Cuerda-Correa *et al*., 2020). A solution could be, as explained by Balsamo *et al*. (2021), the combination with other materials such as graphene, one of the most promising compounds due to its acidic and basic inertness, good flexibility, large area and excellent charge carrier mobility and improving its photocatalytic capabilities. Often, graphene is reduced (rGO) to facilitate interaction with the TiO_2 surface and the reduction is achieved by heat treatment or solar photoreduction.

The production, consumption and disposal of engineered nanoparticles in such quantity and diversity of products inevitably lead to their release into the environment, where they can also pose a risk to

humans; furthermore, it has already been knew that, once in contact with the marine environment, engineered nanoparticles are modified by a series of processes, including at a chemical level through redox reactions (e.g. pH and salinity differences of seawater affect dissolution and aggregation of nanomaterilas) and their effect on the marine environment and life is still unknown (Fairbairn *et al*., 2011).

Some studies have evaluated the toxicity of the most common nanoparticles such as ZnO, Ag and TiO_2 on spermatozoa, larvae and adults of the sea urchins (Fairbairn *et al*., 2011), in particular of *Paracentrotus lividus* (Lamarck, 1816) species, demonstrating toxic effects that dramatically affect the survival rate of embryos (Manzo *et al*., 2013, 2017).

An interesting study carried out on *P. lividus* was performed by Gambardella *et al*. (2013) whose conclusions highlight a toxic effect of TiO_2 nanoparticles exerted on the plutei of *P. lividus*. However, in the literature there are still no data on the effects caused by these newly synthesized nanomaterials and in particular their combinations (such as TiO_2-rGO and TiO_2 sol-gel type) on the vitality and motility of the spermatozoa of this model organism.

3.3 - Materials and methods

3.3.1 - Experimental section

A total of 10 sea urchins *Paracentrotus lividus* used for the experiments were collected by local fishermen in May 2022 and transported in sea water coolers to the laboratory of the University of Catania. Seven on all specimens collected were mature males and were selected after careful stereomicroscopic observation of the genital papillae present on the five plates of the aboral surface (see this non-invasive method at page 11), so only male specimens were used for experimental purpose releasing female specimens. Inside the cavity of their bodies 0.5-1 ml of KCl at 0.5 M were inoculated so that the osmotic shock caused the release of gametes (Fig. 29). The stock solution was centrifugated at 2.000 rpm for 1 min and subsequently 20 µl of sperm pellets was diluted in 1980 µl (final rate of 1:100) (Fabbrocini *et al*., 2016) of in filtered sea water (temp: 20 ± 1 °C, pH: 8,1 ± 0.05, psu: 37 ± 1 ‰), obtained using 0.22 µm filters. The gametes have been preliminarily observed under a microscope to evaluate their quality and before carrying out the experiments, both the vitality and the motility of the samples obtained were evaluated, finding a percentage greater than 70-80%.

Fig. 29: Sperm release of *P. lividus* in 150 ml beacker after 0.5 M of KCl inoculation (by Sara Ignoto).

3.3.2 - Synthesis and characterizations of TiO_2-rGO and TiO_2 sol-gel NPs

TiO_2 nanocomposites used for the experiments were provided by CNR-IMM of University of Catania. Thanks to its good photocatalytic properties and easy preparation, titanium dioxide (TiO_2) is the most employed semiconductor in environmental remediation and water purification. Graphenic structures are the most promising materials that can be efficiently combined with TiO_2, thanks to their excellent charge carrier mobility, acid and basic inertness, good flexibility, and considerably large specific surface area (Rodriguez *et al*., 2021). The standard hydrosolvothermal synthesis of TiO_2-rGO (titanium oxide-reduced graphene oxide) composites requires high temperatures and several steps. However, it was used a one-pot preparation that allowed us to obtain the photocatalysts with a simple and green procedure: the exploiting of the photocatalytic properties of titania were activated by solar irradiation (Balsamo *et al*., 2021). This method allowed us to obtain a more active composite of TiO_2-rGO (1%) (Fig. 30a) compared to those obtained with the standard method (thermal route). The second nanocomposite used it was synthesized by another method that use the sol-gel process. Although in the first phase of their development, imprinted sol-gel materials went unnoticed, in more recent times the introduction of molecular imprinting in synthetic polymers triggered a new interest in the field. The sol-gel process concerns the creation of an oxide network by progressive

polycondensation reactions of molecular precursors in a liquid medium. The process starts with low molecular weight organic solution of monomeric, metal or semimetal alkoxide precursors $M(OR)_n$, where M represents a network-forming element such as Si, Ti, Zr, Al, B, etc., and R is typically an alkyl group (CxH2x þ 1) and water. Generally, both the hydrolysis and condensation reactions occur simultaneously once the hydrolysis reaction has been initiated. During the sol-gel transformation, the viscosity of the solution gradually increases as the sol (colloidal suspension of very small particles, 1–100 nm) becomes interconnected to form a rigid, porous network-the gel (Fig. 30b). Metal alkoxides of titanium, zirconium, tin or aluminum are much more reactive towards water than alkoxysilanes due to the lower electronegativity and higher Lewis's acidity. During drying, alcohol and water evaporate from the pores causing the gel to shrink. Xerogels (fully dried gels) are significantly less porous than their hydrated counterparts. The chemical reactions that take place during the formation of the sol, gel and xerogel strongly influence the properties and composition of the final material (Diaz-Garcìa and Badìa-Laìño, 2005).

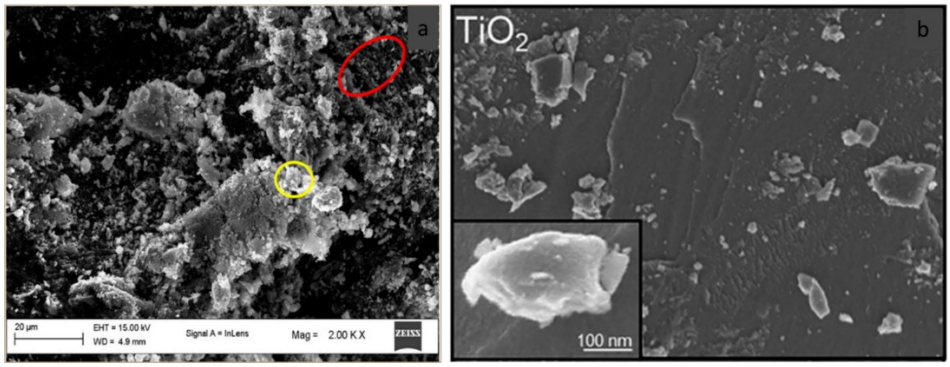

Fig. 30: a) SEM images of TiO_2-rGO at 2K magnification. (Balsamo *et al*., 2021). Scale bar = 20 µm; b) SEM images of TiO_2 sol-gel (Fiorenza *et al*., 2020). Scale bar = 100 nm.

3.3.3 - Preparation of TiO_2-rGO and TiO_2 sol-gel NPs solutions

Two stock concentrations were carried out respectively with the nanocompounds TiO_2-rGO and TiO_2 sol-gel in filtered seawater (0.22 µm filters). The solutions thus obtained were sonicated (3 cycles of 3 minutes each; frequency 40 kHz) to guarantee a homogeneous dispersion of the nanoparticles and were then resuspended by vortexing before each use. Dilutions were obtained from the stock concentrations, so spermatozoa were exposed to both experimentations to 10, 20 and 40 µg/ml of

TiO_2-rGO and TiO_2 sol-gel for two different exposure times: 30 and 60 minutes. For both spermiotoxicity assays 3 replicates were performed for each concentration tested.

3.3.4 - Vitality Analysis

For each replicate it was evaluated the viability of spermatozoa using the eosin test (Lin *et al*., 1998): the cell membrane of non-viable spermatozoa exposed to the dye eosin (ratio 1:1) breaks down thus allowing the passage of the dye, so dead sperm appear fully or partially coloured pink, while live sperm have no colour. The slides were prepared with 10 µl of sperm sample which was added 10 µl of Eosin Y (0.5% v/v, Bio-Optica) and finally covered with a coverslip. The slides were observed under an optical microscope (Leica DMLB) at x100 magnification equipped with a camera. At least 200 sperm cells were counted in five different fields.

3.3.5 - Motility Analysis

The evaluation of the motility was carried out through observations under the optical microscope (Leica DMLB) at x40 magnification. For each replicate of the time series exposure, a 10 µl of sperm sample was placed on a glass slide and covered with a coverslip. Spermatozoa were classified into motile (progressive and non-progressive) and immobile. At least 200 spermatozoa were considered in five different observation fields.

3.3.6 - Statistical Analysis

Statistical data was analysed using GraphPad Prism software (version 9.3.1) and the same software was used to create the graphs. The difference between variances was analysed by two-way ANOVA, followed by Tukey's hoc test for differences between groups. The level of significance was set at $p<0.05$. All data were represented as mean ± standard deviation (SD). Statistically significant data were indicated with a symbol (*$p<0.05$ and **$p<0.01$).

3.4 - Results and discussions

3.4.1 - Spermiotoxicity test with TiO_2-rGO

Mortality rates in all replicates were obtained from non-viable sperm counts in the five reading fields for each slide. The images below (Fig. 31 a,b,c,d) show examples of fields examined under the optical microscope after 30 minutes of exposure to concentrations of 10 µg/ml, 20 µg/ml and 40 µg/ml of TiO_2-rGO: it was possible to observe as the percentage of mortality of the spermatozoa presents higher values as the exposure concentration of the nanocompound increases.

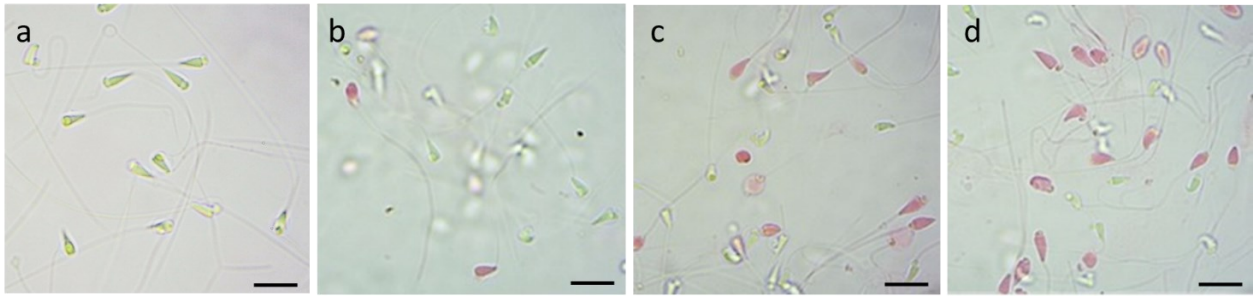

Fig. 31: Vitality evaluation with Eosin Test on *P. lividus* spermatozoa exposed to TiO_2-rGO for 30 minutes: a) CTRL group; b) spermatozoa exposed to 10 µg/ml; c) spermatozoa exposed to 20 µg/ml; d) spermatozoa exposed to 40 µg/ml. Scale bar a,b,c,d = 5 µm (by Sara Ignoto).

The following figure (Fig. 32) shows the percentages of vitality of *P. lividus* spermatozoa exposed to the TiO_2-rGO nanocompound both at 30 and at 60 minutes of exposure. Through the two-way ANOVA test, it was possible to state that there is a highly significant statistical difference (** $p < 0.01$) between the control group and the exposed groups for all concentrations and exposure times.

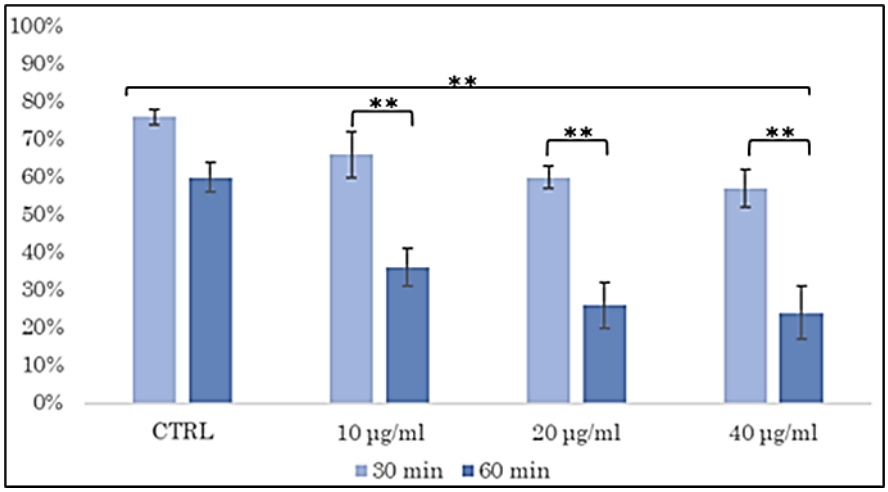

Fig. 32: Vitality rate of *P. lividus* sperm exposed to TiO_2-rGO at concentrations of 10, 20 and 40 µg/ml for 30 and 60 minutes. CTRL= control. *p value < 0.05; ** p value < 0.01.

Therefore, it can be deduced that TiO_2-rGO has a toxic effect on *P. lividus* sperm at the tested concentrations. The viability of male gametes at concentrations of 10, 20 and 40 µg/ml after 30 minutes was reduced showing the respective values of 66%, 60% and 57%; after 60 minutes of exposure the vitality drastically reduced showing the respective values of 36%, 26% and 24% with respect to the control group (CTRL) which showed a percentage of vitality equal to 76% after 30 minutes and 60% after 60 minutes of exposure: thus suggesting the vitality of the spermatozoa is compromised by concentration of the nanocompound and in particular by the times of exposure.

Furthermore, sperm motility is also influenced by presenting very low percentages since exposure to 30 minutes (Fig. 33), especially at the highest concentrations of the nanocompound: in particular, at the respective exposure concentrations (10, 20 and 40 µg/ ml) motility was reduced to 68%, 41% and 28%; while after 60 minutes of exposure the vitality decreases presenting the respective values of 65%, 34% and 21%, with respect to the control group (CTRL) which showed a percentage of vitality equal to 76% after 30 minutes and 78% after 60 minutes of exposure.

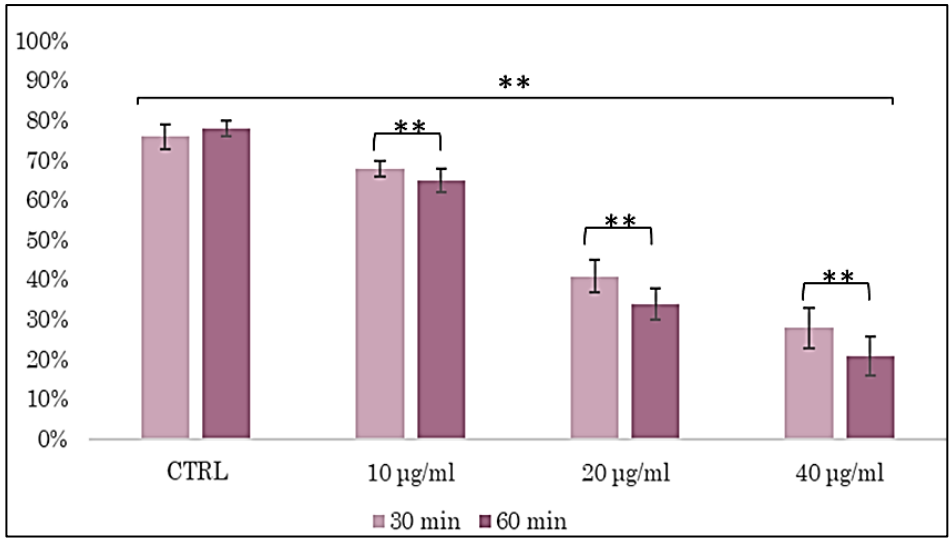

Fig. 33: Motility rate of *P. lividus* sperm exposed to TiO_2-rGO at concentrations of 10, 20 and 40 µg/ml for 30 and 60 minutes. CTRL= control. *p value < 0.05; ** p value < 0.01.

3.4.2 - Spermiotoxicity test with TiO_2 sol-gel

Through the eosin test, the respective percentages of mortality in the performed replicas were calculated. The images below (Fig. 34 a,b,c) are examples of fields examined under the optical microscope which show how after 30 minutes of exposure to concentrations of 10, 20 and 40 µg/ml of TiO_2 sol-gel it is possible to observe, as TiO_2-rGO nanocompound, a higher percentage of mortality of the spermatozoa as the exposure concentration of the nanoparticle increases.

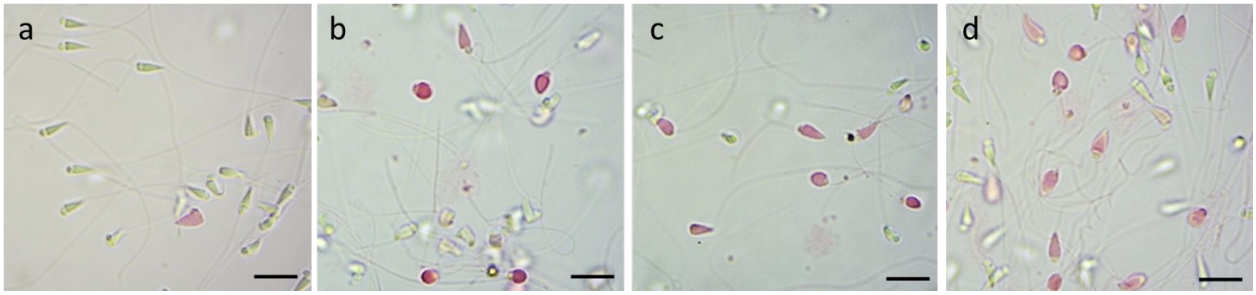

Fig. 34: Vitality evaluation with Eosin Test on *P. lividus* spermatozoa exposed to TiO_2 sol-gel for 30 minutes: a) CTRL group; b) spermatozoa exposed to 10 µg/ml; c) spermatozoa exposed to 20 µg/ml; d) spermatozoa exposed to 40 µg/ml. Scale bar a,b,c,d = 5 µm (by Sara Ignoto).

The figure below (Fig. 35) shows the percentages of vitality of *P. lividus* spermatozoa exposed to the TiO_2 sol-gel nanoparticle, at 30 and 60 minutes of exposure. Through the two-way ANOVA test, it is possible to state that there is a highly significant statistical difference (** $p < 0.001$) between the control group and the exposed groups for all the concentrations used while there is a statistical significance (* $p < 0.05$) for exposure times.

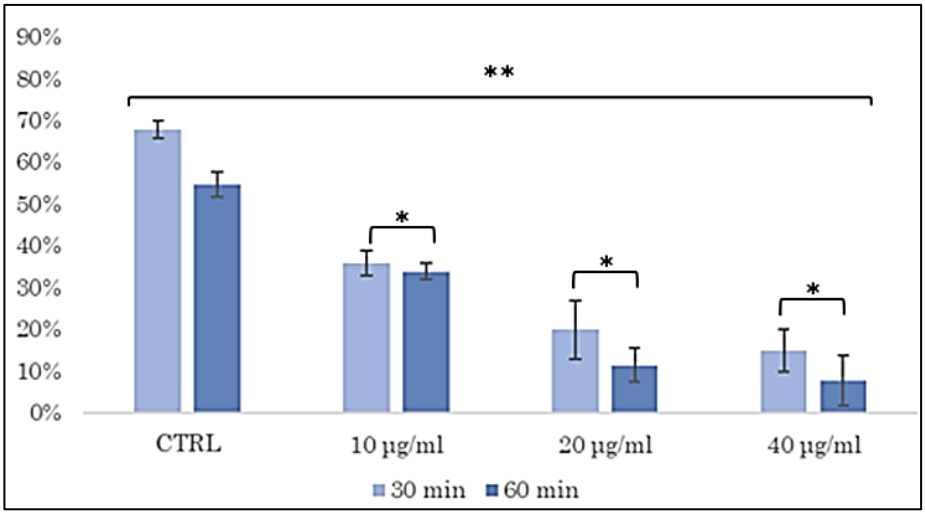

Fig. 35: Vitality rate of *P. lividus* sperm exposed to TiO_2 sol-gel at concentrations of 10, 20 and 40 µg/ml for 30 and 60 minutes. CTRL= control. *p value < 0.05; ** p value < 0.01.

The obtained results show that also the TiO_2 sol-gel has toxic effects on *P. lividus* spermatozoa. However, the toxicity of this nanomaterial depends more on the concentration used than on the exposure times: sperm vitality after 30 minutes of exposure to concentrations of 10, 20 and 40 µg/ml drastically decreases and the percentages are respectively 36%, 20% and 15%, compared to the control (CTRL) which presents a percentage of vitality equal to 68%. From the 60 minute exposure it can be seen that at the concentration of 10 µg/ml, the vitality is 34%; at the concentration of 20 µg/ml it decreases to 12% and is 8% at the concentration of 40 µg/ml of TiO_2 sol-gel, while the percentage of vitality of the control sample spermatozoa (CTRL) is 55%.

For the motility (Fig. 36) of the spermatozoa exposed to the TiO_2 sol-gel, also in this case there is an evident reduction starting from the 30 minutes of exposure; at the lowest exposure concentration (10 µg/ml) the percentage of motility is 35%, while that of the control group (CTRL) has a value equal to 59%; concentrations of 20 µg/ml and 40 µg/ml follow, which present a motility percentage of 27% and 22%, respectively. At 60 minutes of exposure, as the concentrations increase, the percentage of

motile spermatozoa decreases and the percentage of motility is respectively 23%, 21% and 20%, while for the control sample a percentage equal to 51% is recorded.

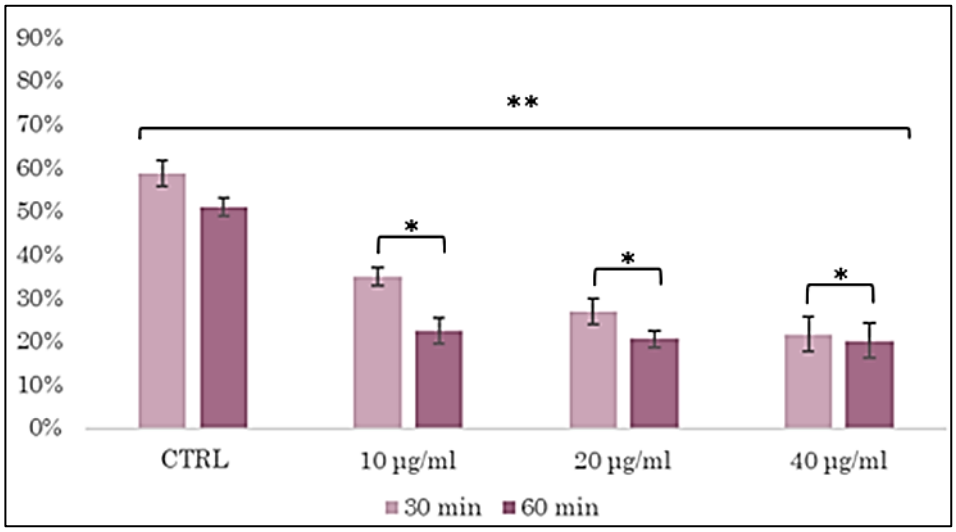

Fig. 36: Motility rate of *P. lividus* sperm exposed to TiO_2 sol-gel at concentrations of 10, 20 and 40 µg/ml for 30 and 60 minutes. CTRL= control. *p value < 0.05; ** p value < 0.01.

3.4.3 - Comparison of spermiotoxicity tests performed

The data obtained from both experiments on *Paracentrotus lividus* spermatozoa showed similar results between the two tested nanomaterials, as in both tests a considerable sensitivity on the part of the spermatozoa was highlighted, which led to a reduction in vitality and motility at all concentrations and exposure times tested (Tab. 5).

	TiO_2-rGO	TiO_2 sol-gel	TiO_2-rGO	TiO_2 sol-gel
	30 minutes		60 minutes	
VITALITY				
CTRL	0,76 ± 0.02	0,68 ± 0.02	0,60 ± 0.04	0,55 ± 0.02
10 µg/ml	0,66 ± 0.06	0,36 ± 0.02	0,36 ± 0.06	0,34 ± 0.04
20 µg/ml	0,60 ± 0.03	0,20 ± 0.04	0,26 ± 0.05	0,12 ± 0.02
40 µg/ml	0,57 ± 0.05	0,15 ± 0.05	0,24 ± 0.07	0,08 ± 0.03
MOTILITY				
CTRL	0,76 ± 0.03	0,59 ± 0.03	0,78 ± 0.03	0,51 ± 0.02
10 µg/ml	0,68 ± 0.02	0,35 ± 0.03	0,65 ± 0.03	0,23 ± 0.07
20 µg/ml	0,41 ± 0.04	0,27 ± 0.05	0,34 ± 0.02	0,21 ± 0.04
40 µg/ml	0,28 ± 0.04	0,22 ± 0.04	0,21 ± 0.05	0,20 ± 0.03

Tab. 5: Comparison of the vitality and motility rates of *P. lividus* sperm exposed to TiO_2-rGO and TiO_2 sol-gel at concentrations of 10, 20 and 40 µg/ml for 30 and 60 minutes. CTRL= control groups.

Specifically, observing the percentages of vitality and motility obtained, it is possible to state that the toxicity of TiO_2-rGO is more significant as the exposure time increases than with the concentration; therefore, it is understood that it is the prolonged exposure to damage the spermatozoa the most.

On the other hand, exposure to TiO_2 sol-gel determined a higher mortality already after 30 minutes of exposure, thus showing a high toxicity more for the tested concentrations than the exposure time. As can be seen from the data, the TiO_2 sol-gel caused a considerable immobility and mortality at the concentration of 10 μg/ml compared to the percentage obtained by TiO_2-rGO, but if the exposure of the latter were prolonged to 60 minutes it would cause the same mortality rates as the first nanomaterial. Therefore, both nanomaterials cause both mortality and immobility of the sperms of the tested model organism.

Although the nanocompounds used are newly synthesized, presenting associated molecular complexes (TiO_2-rGO) and different synthesis phases (TiO_2 sol-gel), the results obtained are in agreement with the data present in the literature in which it has been observed that TiO_2 uncomplexed, at the same concentrations, influenced the fertilization and development of exposed *P.lividus* larvae (Gambardella *et al*., 2013).

3.5 - Conclusion

The presence of emerging contaminants in marine waters is an increasingly worrying and alarming problem: the detection in traces of nanoparticles used for both industrial and domestic purposes is becoming more frequent. TiO_2 is a nanoparticle that is used in numerous applications such as pharmaceuticals and cosmetics, but also to produce paints, paper and plastic material (Macwan *et al*., 2011) and has recently been validated as an excellent photocatalyst in the purification of wastewater, particularly when it is complexed with other compounds such as graphene, but the uncontrolled release could affect the marine ecosystem in which it is poured.

This study carried out on *Paracentrotus lividus* spermatozoa evaluated the effects caused by exposure of male gametes to 10, 20, 40 μg/ml of TiO_2-rGo and TiO_2 sol-gel for 30 and 60 minutes. The results obtained show a significant reduction in the vitality and motility of the spermatozoa at all concentrations and exposure times for both nanomaterials used. This study is a first preliminary work for these newly synthesized materials that confirm the toxic effects of these nanomaterials used on the male gametes of the sea urchin *P. lividus*. Therefore, it will be necessary to deepen the studies on the possible effects on fertilization and the first stages of development of this species which, as we

have already said, is threatened by various xenobiotics and contaminants present in the marine environment.

In conclusion, it can be deduced that the application of TiO_2 in the context of water remediation could represent an excellent solution, however it would be advisable to carry out further studies in order to evaluate the concentration of nanoparticles dispersed in the marine environment which could affect reproduction and development of many organisms.

CHAPTER 4 - GENERAL CONCLUSIONS

Paracentrotus lividus is an emblematic species although several urban activities, such as water pollution, global change and, especially overfishing, threat the existence of this economically relevant species. Hence, the need to adopt new ways in order to mitigate impacts from human activities. In this regard, the development of an efficient echinoculture of the species can help to manage the conservation of this species, not only by a culture totally independent from the natural environment (reduction of fishing pressure) but also, and maybe especially, with plans of restocking.

This research is a contribution to the knowledge of different aspect of this ecologically and economically important species. Indeed, several studies have already proved as this species cover a key role in structuring habitat and ecosystems in coastal areas; furthermore it represents an economical resource for several fishermen (legal and not). On the other hand, the use of sea urchin as model organisms in several fields of the biology was clearly showed and accepted from the scientific community. This research demonstrates the ability of the species to bioaccumulate heavy metals and micronutrients of human and ecosystem concern. The use as bioindicator of the sperm (but also of early stage) of the species resulted of potential utility in order to evaluate due to their sensitivity to different pollutants. For example, the effects of nanoparticles used in water remediation and that are inevitably released in the marine environment, whose effects are little know and could have deleterious effects on marine life, in particular destroying or altering reproductive mechanisms in marine organisms.

In this regard, from the results obtained on the evaluation of the state of maturity of the gonads it is possible to state that only the S3, showed mature individuals in accordance with the widely described reproductive cycle of *P. lividus*. This could be attributed to the fact that S3 is a Nature reserve, therefore less subject to fishing pressures and to all those favourable environmental conditions that a MPA can guarantee, such as the integrity of the habitats which involves, for example, the abundant presence of food sources or greater resistance to changes in environmental parameters.

In fact, much still needs to be done to better understand several aspects about the biology and ecology of the species. In particular, great attention should be paid to the management and protection of the species from legal and illegal fishing activities; to better understand the reproductive biology and development in captivity in order to reach an efficient echinoculture with positive consequences that can derive from it: breeding for human consumption; investments in the production of new biomaterials useful for human health and welfare and other applications; biomedical studies; biomonitoring and restocking in critical areas.

This manuscript provides new data on bioaccumulation, ecotoxicology and reproductive biology aspects of *P. lividus* in the Ionian coast of Sicily, an area in which studies on these aspects are lacking. Further studies with a larger extension on spatio-temporal scale, could provide interesting insights on this relevant species. Indeed, as mentioned above, the importance to deepen our knowledge on this species is of great importance for several fields, from the ecological one, to studies of human concern. Special attention should be paid in the correct management and protection of this species from legal and illegal fishing activities, since in last years the species undergone a considerable decrease in abundance and distribution.

CHAPTER 5 - REFERENCES

Agca Y., Critser J.K. (2002). Cryopreservation of spermatozoa in assisted reproduction. Seminars in Reproductive Medicine, 20, 15-23.

Ahmed S.F., Mofijur M., Nuzhat S., Chowdhury A.T., Rafa N., *et al*. (2021). Recent developments in physical, biological, chemical, and hybrid treatment techniques for removing emerging contaminants from wastewater. Journal of hazardous materials, 416, 125912.

Angioni A., Cau A., Secci M., Addis P. (2014). GC-ITMS analysis of PAH contamination levels in the marine sea urchin *Paracentrotus lividus* in Sardinia. Marine Pollution Bulletin, 82, 201-207.

Arizza V., Giaramita F.T., Parrinello D., Cammarata M., Parrinello N. (2007). Cell cooperation in coelomocyte cytotoxic activity of *Paracentrotus lividus* coelomocytes. Comparative Biochemistry and Physiology Part A: Molecular & Integrative Physiology, 147(2), 389-394.

Arizza V., Vazzana M., Schillaci D., Russo D., Giaramita F.T., *et al*. (2013). Gender differences in the immune system activities of sea urchin *Paracentrotus lividus*. Comparative Biochemistry and Physiology Part A: Molecular & Integrative Physiology, 164(3), 447-455.

Asahina E., Takahashi T. (1978). Freezing tolerance in embryos and spermatozoa of the sea urchin. Cryobiology, 15, 122-127.

Asahina E., Takahashi T. (1979). Cryopreservation of sea urchins and sperm. Development, Growth & Differentiation, 21, 423-430.

Asnaghi V., Collard M., Mangialajo L., Gattuso J. P., Dubois P. (2019). Bottom-up effects on biomechanical properties of the skeletal plates of the sea urchin *Paracentrotus lividus* (Lamarck, 1816) in an acidified ocean scenario. Marine environmental research, 144, 56-61.

Axiak V. and Saliba L.J. (1981). Effects of surface and sunken crude oil on the behaviour of a sea urchin. Marine Pollution Bulletin, 12(1), 14-19.

Balsamo S.A., Fiorenza R., Condorelli M., Pecoraro R., Brundo M.V., Lo Presti F., Sciré, S. (2021). One-pot synthesis of TiO_2-rGO photocatalysts for the degradation of groundwater pollutants. Materials, 14(20), 5938.

Bankhead P. (2014). Analyzing fluorescence microscopy images with ImageJ. ImageJ, 1, 10-1109.

Barnes R.D. (1987). Invertebrate zoology. Saunders College Publishing, Philadelphia. Basuyaux O., Blin J.L. 1998. Use of maize as a food source for sea urchins in a recirculating rearing system. Aquaculture International, 6, 233-247.

Bartley D.M., Bell J.D. (2008). Restocking, stock enhancement, and sea ranching: arena of progress. Rev. Fish. Sci., 16, 357-365.

Bazzardi R., Fattaccio M., Scalza S., Canu A., Marongiu E., Pisanu M. (2014). Preliminary study on Norovirus, hepatitis A virus, *Escherichia coli* and their potential seasonality in shellfish from different growing and harvesting areas in Sardinia region. Italian Journal of Food Safety, 3, 3-8.

Bella J., Paredes E. (2011). Advances in the cryopreservation of sea-urchin embryos: Potential application in marine water quality assessment. Cryobiology, 62, 174-180.

Bertocci I., Blanco A., Franco J.N., Fernàndez-Boo S., Arenas F. (2018). Short-term variation of abundance of the purple sea urchin, *Paracentrotus lividus* (Lamarck, 1816), subject to harvesting in northern Portugal. Marine Environmental Research, 141, 247-254.

Birkeland C. (1989). The influence of echinoderms on coral-reef communities. Echinoderm studies, 3, 1-79.

Bonaviri C., Fernàndez T.V., Badalamenti F., Gianguzza P., Di Lorenzo M., Riggio S. (2009). Fish versus starfish predation in controlling sea urchin populations in Mediterranean rocky shores. Marine Ecology Progress Series, 382, 129-138.

Bonaviri C., Gianguzza P., Pipitone C., Hereu B. (2012). Micropredation on sea urchins as a potential stabilizing process for rocky reefs. Journal of Sea Research, 73, 18-23.

Boudouresque C.F., Verlaque M. (2020). *Paracentrotus lividus* in Developments in Aquaculture and Fisheries Science, London, United Kingdom, 447-485.

Boudouresque C.F., Verlaque M., Azzolina J.F., *et al*. (1989). Evolution des populations de *Paracentrotus lividus* et d'*Arbacia lixula* (Echinoidea) le long d'un transect permanent a` Galeria (Corse). Trav. Sci. Parc Nat. Re´g. Re´s. Nat. Corse 22, 65-82.

Brundu G., Cannavacciuolo A., Nannini M., Somma E., Munari M., Zupo V., Farina S. (2023). Development of an efficient, non-invasive method for identifying gender year-round in the sea urchin *Paracentrotus lividus*. *Aquaculture*, 739082.

Byrne M. (1990). Annual reproductive cycles of the commercial sea urchin *Paracentrotus lividus* from an exposed intertidal and a sheltered subtidal habitat on the west coast of Ireland. Marine Biology, 104(2), 275-289.

Carballeira C., Ramos-Gomez J., Martin-Dìaz L., Del Valls T.A. (2012). Identification of specific malformations of sea urchin larvae for toxicity assessment: application to marine pisciculture effluents. Marine Environmental Research, 77, 12-22.

Carboni S. (2013). Research and development of hatcherytechniques to optimise juvenile production of the edible Sea Urchin, *Paracentrotus lividus*. PhD thesis, University of Stirling, pp. 298.

Carboni S., Hughes A.D., Atack T., Tocher D.R., Migaud H. (2015). Influence of broodstock diet on somatic growth, fecundity, gonad carotenoids and larval survival of sea urchin. Aquaculture Research, 46(4), 969-976.

Carboni S., Vignier J., Chiantore M., Toucher D.R., Migaud H. (2012). Effects of dietary microalgae on growth, survival and fatty acid composition of sea urchin *Paracentrotus lividus* throughout larval development. Aquaculture, 325, 250-258.

Chia F.S., Xing J. (1996). Echinoderm coelomocytes. Zoological Studies Taipei, 35, 231-254.

Chiaramonte M., Inguglia L., Vazzana M., Deidun A., Arizza V. (2019). Stress and immune response to bacterial LPS in the sea urchin *Paracentrotus lividus* (Lamarck, 1816). Fish & Shellfish Immunology, 92, 384-394.

Cuerda-Correa E.M., Alexandre-Franco M.F., Fern´andez-Gonz´alez C. (2020). Advanced oxidation processes for the removal of antibiotics from water. An overview. Water 12, 102.

Davidson E.H., Cameron R.A., Ransick A. (1998). Specification of cell fate in the sea urchin embryo: summary and some proposed mechanisms. Development, 125, 3269-3290.

De Oliveira M., Frihling B.E.F., Velasques J., Magalhães Filho F.J.C., Cavalheri P.S., Migliolo L. (2020). Pharmaceuticals residues and xenobiotics contaminants: occurrence, analytical techniques and sustainable alternatives for wastewater treatment. Science of the Total Environment, 705, 135568.

Devin M.G. (2002). Land-based echinoculture: a novel system to culture adult sea urchins. In: Yokota Y., Matranga V., Smolenicka Z. The sea urchin: from basic biology to aquaculture. Swets & Zeitlinger B.V., Lisse, 145-159.

Di Benedetto C., Barbaglio A., Martinello T., Alongi V., Fassini D., *et al*. (2014). Production, characterization and biocompatibility of marine collagen matrices from an alternative and sustainable source: The sea urchin *Paracentrotus lividus*. Marine Drugs, 12, 4912-4933.

Díaz-Balzac C.A., García-Arrarás J.E. (2018). Echinoderm nervous system. In Oxford research encyclopedia of neuroscience.

Diaz-Garcìa M.E., Badìa-Laìño R. (2005). Molecular imprinting in sol-gel materials: Recent developments and applications. Microchim. Acta, 149, 19-36.

Directive 2000/60/EC. Water Framework Directive.

Directive 2008/56/EC. Marine Strategy Framework Directive.

Ezhova O.V., Malakhov V.V. (2021). The Axial Complex of Echinoderms Represents the Kidney and Is Homologous to the Hemichordate Heart-Kidney. Paleontological Journal, 55(9), 1029-1038.

Ezhova O.V., Malakhov V.V., Egorova E.A. (2018). Axial complex and associated structures of the sea urchin *Strongylocentrotus pallidus* (Sars, G.O. 1871) (Echinodermata: Echinoidea). Journal of Morphology, 279, 792-808.

Fabbrocini A., D'Adamo R. (2010). Gamete maturation and gonad growth in fed and starved sea urchin *Paracentrotus lividus* (Lamarck, 1816), J. Shell. Res. 29(4), 1-9.

Fabbrocini A., D'Adamo R., Del Prete F., Maurizio D., Specchiulli A., Oliveira L.F., Sansone G. (2016). The sperm motility pattern in ecotoxicological tests. The CRYO-Ecotest as a case study. Ecotoxicology and Environmental Safety, 123, 53-59.

Fabbrocini A., D'Adamo R., Pelosi S., Oliveira L.F.J., Silvestri F., Sansone G. (2014). Gamete cryobanks for laboratory research: Developing a rapid and easy-to-perform protocol for the cryopreservation of the sea urchin *Paracentrotus lividus* (Lmk, 1816) spermatozoa. Cryobiology, 69, 149-156.

Fairbairn E.A., Keller A.A., Mädler L., Zhou D., Pokhrel S., Cherr G.N. (2011). Metal oxide nanomaterials in seawater: linking physicochemical characteristics with biological response in sea urchin development. Journal of hazardous materials, 192(3), 1565-1571.

Fernandez C., Boudouresque C. (2000). Nutrition *P. lividus* artificial food. Mar. Ecol. Prog. Ser., 204, 131-141.

Fernandez N., Beiras R. (2001). Combined toxicity of dissolved mercury with copper, lead and cadmium on embryogenesis and early larval growth of the *Paracentrotus lividus* sea-urchin. Ecotoxicology, 10, 263-271.

Ferrario C., Leggio L., Leone R., Di Benedetto C., Guidetti L., *et al*. (2017). Marine-derived collagen biomaterials from echinoderm connective tissues. Marine environmental research, 128, 46-57.

Ferrario C., Sugni M., Somorjai I.M., Ballarin L. (2020). Beyond adult stem cells: dedifferentiation as a unifying mechanism underlying regeneration in invertebrate deuterostomes. Frontiers in Cell and Developmental Biology, 8, 587320.

Fiorenza R., Di Mauro A., Cantarella M., Iaria C., Scalisi E.M. *et al*. (2020). Preferential removal of pesticides from water by molecular imprinting on TiO_2 photocatalysts. Chemical Engineering Journal, 379, 122309.

Flammang P., Gosselin P., Jangoux M. (1998). The podia, organs of adhesion and sensory perception in larvae and post-metamorphic stages of the echinoid *Paracentrotus lividus* (Echinodermata). Biofouling, 12, 161-171.

Formery L., Wakefield A., Gesson M., Toisoul L., Lhomond G., *et al*. (2022). Developmental atlas of the indirect-developing sea urchin *Paracentrotus lividus*: From fertilization to juvenile stages. Front. Cell. Dev. Biol., published online.

Formery L., Orange F., Formery A., Yaguchi S., Lowe C.L., Schubert M., Croce J.C. (2021). Neural anatomy of echinoid early juveniles and comparison of nervous system organization in echinoderms. J Comp Neurol, 529, 1135-1156.

Gago J., Range F., Luis O. (2003). Growth, reproductive biology and habitat selection of the sea urchin *Paracentrotus lividus* in the coastal waters of Cascais, Portugal. In Echinoderm Research, 1st ed.; Feral J.P., David B., Eds.; Balkema: Lisse, The Netherlands, 269-276.

Gambardella C., Aluigi M.G., Ferrando S., Gallus L., Ramoino P., Gatti A.M., Falugi C. (2013). Developmental abnormalities and changes in cholinesterase activity in sea urchin embryos and larvae from sperm exposed to engineered nanoparticles. Aquatic toxicology, 130, 77-85.

Gambarella C., Marcellini F., Falugi C., Varrella S., Corinaldesi C. (2021). Early-stage anomalies in the sea urchin (*Paracentrotus lividus*) as bioindicators of multiple stressors in the marine environment: Overview and future perspectives. Environmental Pollution, 287, 117608.

Gao D., Critser J.K. (2000). Mechanisms of cryoinjury in living cells. ILAR Journal, 41, 187-196.

Garner S., Zysk, I., Byrne G., Kramer M., Moller D., Taylor V., Burke R.D. (2016). Neurogenesis in sea urchin embryos and the diversity of deuterostome neurogenic mechanisms. Development, 143, 286-297.

Gharred T., Ezzine I.K., Naija A., Bouali R.R., Jebali J. (2015). Assessment of toxic interactions between deltamethrin and copper on the fertility and developmental events in the Mediterranean Sea urchin, *Paracentrotus lividus*. Environmental Monitoring and Assessment, 187(4), 1-8.

Giordani G., Viaroli P., Swaney D.P., Murray C.N., Zaldivar J.M., Marshland Crossland J.I. (2005). Nutrient fluxes in transitional zones of the Italian coast. LOICZ Reports & Studies, Texel, the Netherlands, 28, pp. 157.

Gosselin P., Jangoux M. (1998). From competent larva to exotrophix juvenile: a morphofunctional study of the perimetamorphic period of *Paracentrotus lividus* (Echinodermata, Echinoida). Zoomorphology, 118, 31-43

graphene oxide and titania loaded nafion membranes in zebrafish. Front Physiol, 8:1039.

Guettaf M., San Martin G.A., Francour P. (2000). Interpopulation variabilty of the reproductive cycle of *Paracntrotus lividus* (Echinodermata: Echinoidea) in the south-western Mediterranean. J. Mar. Biol. Assoc. UK, 80, 899-907.

Gupta S.M., Tripathi M. (2010). A review of TiO_2 nanoparticles, Chinese Science Bulletin, 56, 1639-1657.

Harrold C., Pearse J.S. (1987). The ecological role of echinoderms. Echinoderm studies 2, 2, 137-233.

Hibino T., Loza-Coll M., Messier C., Majeske A.J., Cohen A.H., Terwilliger D.P., Buckley K.M., Brockton V., Nair S.V., Berney K., Fugmann S.D., Anderson M.K., Pancer Z., Cameron R.A., Smith L.C., Rast J.P. (2006). The immune gene repertoire encoded in the purple sea urchin genome. Developmental biology, 300(1), 349-365.

James P., Evensen T., Samuelsen A. (2017). Commercial scale sea urchin roe enhancement in Norway: Enhancement, transport, and market assessment. Tromsø: Nofima AS (ISBN: 978-82-8296-490-6).

Jones O.A.H., Voulvoulis N., Lester J.N. (2004). Potential ecological and human health risks associated with the presence of pharmaceutically active compounds in the aquatic environment. Crit. Rev. Toxicol, 34, 335-350.

Kainz P., Mayrhofer-Reinhartshuber M., Ahammer H. (2015). IQM: an extensible and portable open source application for image and signal analysis in Java. PLoS One 10(1), e0116329.

Kaul-Strehlow S., Urata M., Minokawa T., Stach T., Wanninger A. (2015). Neurogenesis in directly and indirectly developing enteropneusts: Of nets and cords. Organisms Diversity & Evolution,15(2), 405-42.

Kitching J.A., Thain V.M. (1983). The ecological impact of the sea urchin *Paracentrotus lividus* (Lamarck) in Lough Ine, Ireland. Philosophical Transactions of the Royal Society B: Biological Sciences, 300, 513-552.

La Bella G., Martella V., Basanisi M.G., Nobili G., Terio V., La Salandra G. (2017). Food-borne viruses in shellfish: Investigation on norovirus and HAV presence in Apulia (SE Italy). Food and Environmental Virology, 9, 179-186.

Leonelli S., Ankeny R.A. (2013). What makes a model organism? Endeavour, 37, 209-212.

Lin M., Morshedi M., Srisombut C., Nassar A., Oehninger S. (1998). Plasma membrane integrity of cryopreserved human sperm: an investigation of the results of the hypoosmotic swelling test, the water test, and eosin-y staining. Fertility and Sterility, 70(6), 1148-1155.

Lozano J., Galera J., Lòpez S., Turon C., Palacin C, Morera C. (1995). Biological cycles and recruitment of *Paracentrotus lividus* (Echinodermata: Echinoidea) in two contrasting habitats. Marine Ecology Progress Series, 122, 179-191.

Macwan D.P., Dave P.N., Chaturvedi S. (2011). A review on nano-TiO_2 sol–gel type syntheses and its applications. Journal of materials science, 46(11), 3669-3686.

Mantilla-Aldana L., Campoy-López P., Pereira-Pinto E., Beiras R. (2020). Pixelar index: a new quantitative approach for the assessment of reproductive condition in the purple sea urchin, *Paracentrotus lividus*, by image analysis. *Aquaculture International*, 28(2), 841-850.

Manzo S., Miglietta M.L., Rametta G., Buono S., Di Francia G. (2013). Embryotoxicity and spermiotoxicity of nanosized ZnO for Mediterranean Sea urchin *Paracentrotus lividus*. Journal of hazardous materials, 254, 1-9.

Manzo S., Schiavo S., Oliviero M., Toscano A., Ciaravolo M., Cirino P. (2017). Immune and reproductive system impairment in adult sea urchin exposed to nanosized ZnO via food. Science of the Total Environment, 599, 9-13.

Marcos C., Díaz D., Fietz K., Forcada A., Ford A., García-Charton J.A., *et al*. (2021). Reviewing the ecosystem services, societal goods, and benefits of marine protected areas. Frontiers in Marine Science, 8, 613819.

Martinez-Paramo S., Horvath A., Labbé C., Zhang T., Robles V., Herraez P., *et al*. (2017). Cryobanking of aquatic species. Aquaculture, 472, 156-177.

Martino C., Byrne M., Roccheri M.C., Chiarelli R. (2021). Interactive effects of increased temperature and gadolinium pollution in *Paracentrotus lividus* sea urchin embryos: a climate change perspective. Aquat. Toxicol., published online.

Mashanov V.S., Zueva O.R., Rubilar T., Epherra L., Garcia-Arraras J.E. (2016). Echinodermata. In A. Schmidt-Rhaesa S., Harzsch & Purschke G. (Eds.), Structure and Evolution of Invertebrate Nervous Systems, Oxford: Oxford University Press, 665-688.

Mortensen T. (1943). A Monograph of the Echinoidea, III.3 Camarodonta. II. Echinidae, Strongylocentrotidae, Parasaleniidae, Echinometridae. C.A.Reitzel, Copenhagen.

Moss M.L, Meehan M.M. (1967). Sutural connective tissues in the test of an echinoid *Arbacia punctulata*. Acta Anatomica, 66, 279-304.

Murillo-Navarro R.; Jiménez-Guirado D. (2012). Relationships between algal food and gut and gonad conditions in the Mediterranean Sea urchin *Paracentrotus lividus* (Lam.) Mediterranean Marine Science, 13, 227-238.

Naidu R., Espana V.A.A., Liu Y., Jit J. (2016). Emerging contaminants in the environment: risk-based analysis for better management. Chemosphere 154, 350-357.

Nedélec H., Verlaque M. (1984). Alimentation de l'oursin *Paracentrotus lividus* (Lam.) dans un herbier a *Posidonia oceanica* (/L.) Delile en corse (Méditerranée, France). In: Boudouresque C.F., De Grissac J.A., Oliver J. (eds) International workshop on *Posidonia oceanica* beds. Vol 1 GIS Posidonie publ. Porquerolles, 349-364.

Oral R., Pagano G., Siciliano A., Gravina M., Palumbo A., *et al*. (2017). Heavy rare earth elements affect early stages in *Paracentrotus lividus* and *Arbacia lixula* sea urchins. Environmental Research, 154, 240-246.

Ouchene H., Boutgayout H., Hermas J., Benbani A., Abou Oualid J. *et al*. (2021). Reproductive Cycle of Sea Urchin *Paracentrotus lividus* (Lamarck, 1816) from the South Coast of Morocco: Histology, Gonads Index, and Size at First Sexual Maturity. *Arabian Journal for Science and Engineering*, 46(6), 5393-5405.

Ouréns R., Fernandez L., Fernandez-Boan M., Naya I., Freire J. (2013). Reproductive dynamics of the sea urchin *Paracentrotus lividus* on the Galicia coast (NW Spain): Effects of habitat and population density. Marine Biology, 160, 2413-2423.

Paredes E., Adams S.L., Vignier J. (2019). In: *Echinoderms, Part A* (eds.) Foltz K.R., Hamdoun A. Cryopreservation of sea urchin sperm and early life stages. Methods in Cell Biology, 150, 47-69.

Paredes E., Bellas J. (2015). The use of cryopreserved sea urchin embryos (*Paracentrotus lividus*) in marine quality assessment. Chemosphere, 128, 278-283.

Pawson D.L., Pawson D.J., King R.A. (2010). A taxonomic guide to the Echinodermata of the South Atlantic Bight, USA: 1. Sea cucumbers (Echinodermata: Holothuroidea). Zootaxa, 2449(1), 1-48.

Pecoraro R., D'Angelo D., Filice S., Scalese S., Capparucci F., *et al*. (2018). Toxicity evaluation of graphene oxide and titania loaded nafion membranes in zebrafish. Front Physiol, 8, 1039.

Pinna M.G. (2014) The edible sea urchin *Paracentrotus lividus* (Lamarck, 1816): a valuable resource for fisheries and aquaculture purposes in Sardinia (Central western Mediterranean). PhD thesis, University of Sassari, pp. 161.

Piraino S., Fanelli G., Boero F. (2002). Variability of species' roles in marine communities: change of paradigms for conservation priorities. Marine Biology 140, 1067-1074.

Piwowarska D., Kiedrzyńska E. (2021). Xenobiotics as a contemporary threat to surface waters. Ecohydrology & Hydrobiology.

Polge C., Smith A.U., Parkers A.S. (1949). Revival of spermatozoa after vitrification and dehydration at low temperatures. Nature, 164, 666.

Qiao D., Nikitina L.A., Buznikov G.A., Lauder J.M., Seidler F.J., Slotkin T.A. (2003). The sea urchin embryo as a model for mammalian developmental neurotoxicity: ontogenesis of the high-affinity choline transporter and its role in cholinergic trophic activity. Environmental Health Perspectives, 11, 1730-1735.

Rakaj A., Morroni L., Grosso L., Fianchini A., Pensa D., Pellegrini D., *et al*. (2021). Towards sea cucumbers as a new model in embryo-larval bioassays: *Holoturia tubulosa* as test species for the Assessment of Marine Pollution. Sci. Total. Environ., 787, 147593.

Rast J.P., Smith L.C., Loza-Coll M., Hibino T., Litman G.W. (2006). Genomic insights into the immune system of the sea urchin. Science, 314, 952-956.

Rego R.M., Kuriya G., Kurkuri M.D., Kigga M., (2021). MOF based engineered materials in water remediation: recent trends. J. Hazard. Mater. 403, 123605

Reunov A.A., Yurchenko O.V., Kalachev A.V., Au D.W.T. (2004). An ultrastructural study of phagocytosis and shrinkage in nutritive phagocytes of the sea urchin *Anthocidaris crassispina*. Cell Tissue Res, 318, 419-428.

Richner H., Milinski M. (2000). On the functional significance of masking behaviour in sea urchins an experiment with *Paracentrotus lividus*. Marine Ecology Progress Series, 205, 307-308.

Rocha A.C., Camacho C., Eljarrat E., Peris A., Aminot Y., Readman J.W., Boti V., Nannou C., Marques A., Nunes M.L., Almeida C.M. (2018). Bioaccumulation of persistent and emerging pollutants in wild sea urchin *Paracentrotus lividus*. Environmental Research 161, 354-363.

Rodriguez V., Camarillo R., Martinez F., Jimenez C., Rincon J. (2021). High-pressure synthesis of rGO-TiO_2/Cu catalysts for efficient CO2 reduction under solar light. J. Supercrit. Fluids, 174, 105265.

Rodriguez-Narvaez O.M., Peralta-Hernandez J.M., Goonetilleke A., Bandala E.R. (2017). Treatment technologies for emerging contaminants in water: a review. Chem. Eng. J., 323, 361-380.

Rouane-Hacene O., Boutiba Z., Benaissa M., Belhaouari B., Francour P., *et al*. (2018). Seasonal assessment of biological indices, bioaccumulation, and bioavailability of heavy metals in sea urchins *Paracentrotus lividus* from Algerian west coast, applied to environmental monitoring. Environ Sci Pollut Res, 25, 11238-11251.

Ruocco N., Costantini M., Santella L. (2016). New insights into negative effects of lithium on sea urchin *Paracentrotus lividus* embryos. Scientific Reports, 6, 32157.

Sala E. (1997). Fish predators and scavengers of the sea urchin *Paracentrotus lividus* in protected areas of the north-west Mediterranean Sea. Marine Biology, 129, 531-539.

Sala E., Ribes M., Hureu B., Zabala M., Alvà V., Coma R., Garrabou J. (1998). Temporal variability in abundance of the sea urchins *Paracentrotus lividus* and *Arbacia lixula* in the northwestern Mediterranean: comparison between a marine reserve and an unprotected area. Mar. Ecol. Prog. Ser., 168, 135-145.

Salvatore M.M., Ciaravolo M., Cirino P., Toscano A., Salvatore F., Gallo M., Naviglio D., Andolfi A. (2019). Fatty acids from *Paracentrotus lividus* sea urchin shells obtained via rapid solid liquid dynamic extraction (RSLDE). Separations, 6, 50.

Santos P.M., Albano P., Raposo A., Ferreira S.M., Costa J.L., Pombo A. (2020b). The effect of temperature on somatic and gonadal development of the sea urchin *Paracentrotus lividus* (Lamarck, 1816). *Aquaculture*, *528*, 735487.

Santos P.M., Ferreira S.M., Albano P., Raposo A., Costa J. L., Pombo A. (2019). Can artificial diets be a feasible alternative for the gonadal growth and maturation of the sea urchin *Paracentrotus lividus* (Lamarck, 1816)?. Journal of the World Aquaculture Society, 51(2), 463-487.

Santos P.M., Ferreira S.M., Mesquita J.R., Rivadulla E., Inàcio A.S., Nascimento M.S.J., Romalde J., Martins da Costa P. (2020a). Norovirus contamination of sea urchins (*Paracentrotus lividus*): Potential food risk for consumers. Food Control, 111, 107041.

Sartori D., Gaion A. (2016). Can sea urchin benefit from an artificial diet? Physiological and histological assessment for echinoculture feasibility evaluation. Aquacult. Nutr., 22, 1214-1221.

Sartori D., Macchia S., Vitiello V., Morroni L., Onorati F., Pellegrini D. (2017). ISPRA, Quaderni – Ricerca Marina n. 11/2017. A cura di Macchia S., Sartori D., Roma, pp 60.

Savriama Y., Gerber S. (2018). Geometric morphometrics of nested symmetries unravels hierarchical inter-and intra-individual variation in biological shapes. Scientific Reports, 8(1), 1-12.

Savy S. (1987). Les prédateurs de *Paracentrotus lividus* (Echinodermata). In: Boudouresque CF (ed) Colloque International sur *Paracentrotus lividus* et les oursins comestibles. GIS Posidonie, Marseille, 413-423.

Scanu S., Soetebier S., Piazzolla D., Tiralongo F., Mancini E., Romano N., Marcelli M. (2015). Concentrations of As, Cd, Cr, Ni, and Pb in the echinoid *Paracentrotus lividus* on the coast of Civitavecchia, northern Tyrrhenian Sea, Italy. Regional Studies in Marine Science, 1, 7-17.

Schäfer S., Abele D., Weihe E., Köhler A. (2011). Sex-specific biochemical and histological differences in gonads of sea urchins (*Psammechinus miliaris*) and their response to phenanthrene exposure. Marine environmental research, 71(1), 70-78.

Schillaci D., Arizza V., Parrinello N., Di Stefano V., Fanara S., Muccilli V., Cunsolo J.J.A., Haagensen S., Molin S. (2010). Antimicrobial and antistaphylococcal biofilm activity from the sea urchin *Paracentrotus lividus*. Journal of applied microbiology, 108(1), 17-24.

Smith L.C., Ghosh J., Buckley K.M., Clow L.A., Dheilly N.M., *et al*. (2010). Echinoderm immunity. *Invertebrate immunity*, 260-301.

Stefansson G., Kristinsson H., Ziemer N., Hannon C., James P. (2017). Markets for sea urchins: A review of global supply and markets. Technical Report, pp. 45.

Sugni M., Ciappellano S.G., Biressi A.C.M., Fernandes D., Porte C., Candia M.D. (2010). Sexual dimorphism in the sea urchin *Paracentrotus lividus*: morphological and biochemical analysis. In: International Workshop Status and management of the edible sea urchin *Paracentrotus lividus* in Mediterranean Sea: Book of abstracts edited by Mazzola A., Chemello R., Gianguzza P. Palermo: Universita` di Palermo, pp. 44.

Tahara Y., Okada M., Kobayashi N. (1958). Secondary sexual characters in japanese sea-urchins. Publ. Seto Mar. Biol. Lab., 7 (1), 165-172.

Tahara Y., Okada M., Kobayashi N. (1960). Further notes on the sexual dimorphism in japanese sea urchins. Publ. Seto Mar. Biol. Lab., 8 (1), 183-189.

Tervit H.R., Adams S.L., Roberts R.D., McGowan L.T., Pugh P.A., Smith J.F., *et al*. (2005). Successful cryopreservation of Pacific oyster (*Crassostrea gigas*) oocytes. Cryobiology, 51, 142-151.

Tijani J.O., Fatoba O.O., Babajide O.O., Petrik L.F. (2016). Pharmaceuticals, endocrine disruptors, personal care products, nanomaterials and perfluorinated pollutants: a review. Environ. Chem. Lett. 14, 27-49.

Timerbaev A.R., Kuznetsova O.V., Keppler B.K. (2021). Current trends and challenges in analysis and characterization of engineered nanoparticles in seawater. Talanta, 226, 122201.

Tornero A.M., Hanke G. (2017). Potential chemical contaminants in the marine environment: An overview of main contaminant lists. EUR 28925 EN. Publications Office of the European Union: Luxembourg.

Tortonese E. (1965). Echinodermata. Fauna d'Italia VoL.IV. Bologna, Edizioni Calderini.

Trousset J. (1885). Nouveau dictionnaire encyclope´dique universel illustre´: re´pertoire des connaissances humaines, 4, pp. 372.

Turon X., Giribert G., Lopez S., Palacin C. (1995). Growth and population structure *Paracentrotus lividus* (Echinodermata: Echinoidea) in two contrasting habitats. Marine Ecology Progress Series, 122, 193-204.

Unuma T., Ikeda K., Yamano K., Moriyama A., Ohta H. (2007). Zinc-binding property of the major yolk protein in the sea urchin—Implications of its role as a zinc transporter for gametogenesis. FEBS J, 274, 4985-4998.

Vacquier V.D. (2011). Laboratory on sea urchin fertilization. Molecular Reproduction and Development, 78, 553-564.

Vafidis D., Antoniadou C., Kyriakouli K. (2019). Reproductive cycle of the edible sea urchin *Paracentrotus lividus* (Echinodermata: Echinoidae) in the Aegean Sea. *Water*, 11(5), 1029.

Vaschenko M.A., Zhadan P.M., Aminin D.L., Almyashova T.N. (2012). Lipofuscin-Like Pigment in Gonads of Sea Urchin *Strongylocentrotus intermedius* as a Potential Biomarker of Marine Pollution: A Field Study. Arch Environ Contam Toxicol 62, 599-613.

Vizzini S., Visconti G., Signa G., Romano S., Mazzola A. (2019). A new sustainable formulated feed based on discards from food industries for rearing the sea urchin *Paracentrotus lividus* (Lmk.). Aquacult. Nutr., 25, 691-701.

Walker C.W, Harrington L.M., Lesser M.P., Fagerberg W.R. (2005). Nutritive phagocyte incubation chambers provide a structural and nutritive microenvironment for germ cells of *Strongylocentrotus droebachiensis*, the green sea urchin. Biol Bull., 209, 31-48.

Wiesmann V., Franz D., Held C., Münzenmayer C., Palmisano R., Wittenberg T. (2015). Review of free software tools for image analysis of fluorescence cell micrographs. J Microsc, 257(1), 39-53.

WoRMS Editorial Board (2022). World Register of Marine Species. Available from https://www.marinespecies.org at VLIZ. Accessed 2022-12-09.

Ziegler A., Faber C., Bartolomaeus T. (2009). Comparative morphology of the axial complex and interdependence of internal organ systems in sea urchins (Echinodermata: Echinoidea). Frontiers in Zoology, 6(1), 1-31.

Zilia F., Bacenetti J., Sugni M., Matarazzo A., Orsi, L. (2021). From waste to product: Circular economy applications from sea urchin. Sustainability, 13(10), 5427.

Zupo V., Glaviano F., Paolucci M., Ruocco N., Polese G., di Cosmo A., *et al*. (2019). Roe enhancement of *Paracentrotus lividus*: Nutritional effects of fresh and formulated diets. Aquacult. Nutr., 25, 26-38.